

## Cathode Materials for Lithium-ion Batteries: A brief review

Ayodele O. Soge\*, Alexander A. Willoughby, Oluropo F. Dairo, Olubunmi O. Onatoyinbo

Department of Physical Sciences, Faculty of Natural Sciences, Redeemer's University, PMB 230, Ede, Osun State, Nigeria.

\*Corresponding Author Email: [sogea@run.edu.ng](mailto:sogea@run.edu.ng), [ayosoge@gmail.com](mailto:ayosoge@gmail.com)

<https://doi.org/10.14447/jnmes.v24i4.a02>

### ABSTRACT

Received: May 21-2021

Accepted: September 30-2021

**Keywords:** *Lithium-ion batteries, cathode materials, lithium storage, discharge capacity, energy density, cycling performance, lithiation, delithiation*

Layered lithium cobalt oxide (LiCoO<sub>2</sub>) as a pioneer commercial cathode for lithium-ion batteries (LIBs) is unsuitable for the next generation of LIBs, which require high energy density, good rate performance, improved safety, low cost, and environmental friendliness. LiCoO<sub>2</sub> suffers from structural instability at a high level of delithiation and performance degradation when overcharged. Besides, cobalt, a significant constituent of LiCoO<sub>2</sub> is more costly and less environmentally friendly than other transition metals. Therefore, alternative cathode materials are being explored to replace LiCoO<sub>2</sub> as cathode materials for high-performance LIBs. These new cathode materials, including lithiated transition metal oxides, vanadium pentoxides, and polyanion-type materials, are reviewed in this study. The various challenges hampering the full integration of these cathode materials in commercial LIBs and viable solutions are emphasised.

## 1. INTRODUCTION

Lithium-ion batteries (LIBs) are of great significance as power sources to satisfy the increasing demands for clean and sustainable energy systems and low-emission or zero-emission electric vehicles [1],[2]. As a sustainable and promising renewable energy store, LIBs have replaced other types of batteries for many portable consumer electronics, including mobile phones, laptops, and cameras [1]. The dominance of LIBs in the rechargeable battery market segment has been attributed to their large specific capacity, high voltage, high power, high efficiency, and environmental friendliness [3],[4]. For the next generation of LIBs to meet the growing demands of new technologies, they must possess high energy density, good rate performance, improved safety, and low cost [5]. From the materials perspective, the storage capacity and affordability of LIBs are characteristically limited by the cathode. Consequently, developing cost-effective and high-performance cathode materials is an imperative task for advancing LIB technology [6]–[8].

Layered lithium cobalt oxide (LiCoO<sub>2</sub>) is the first commercial cathode for LIBs and has received tremendous attention since its discovery in 1980 [9]–[14]. Although the complete removal of lithium gives a sizeable theoretical capacity of 274 mAh g<sup>-1</sup>, the Li<sub>1-x</sub>CoO<sub>2</sub> structure tends to be unstable at high levels of delithiation, typically when x exceeds 0.5 [9]. Thus, the usable specific capacity of LiCoO<sub>2</sub> is below 150 mAh g<sup>-1</sup> [5]. Apart from being highly toxic, cobalt is less available and more expensive than other transition metals, such as manganese, nickel, and iron [9],[15]. Besides, LiCoO<sub>2</sub> is not as stable as other potential electrode materials and can undergo performance degradation or failure when overcharged [16]–[18]. Therefore, alternative materials are being developed to replace LiCoO<sub>2</sub> as cathode materials for LIBs to reduce cost and improve stability [15]. The alternative

cathode materials being considered as a replacement for LiCoO<sub>2</sub> include layered lithiated transition metal oxides (e.g., LiNi<sub>x</sub>Co<sub>y</sub>M<sub>z</sub>O<sub>2</sub> (x+y+z=1, M=Mn/Al), Mn-based spinels (e.g., LiMn<sub>2</sub>O<sub>4</sub>), vanadium pentoxides, and polyanion-type materials (e.g., phosphates, borates, fluorosulphates, and silicates). The operating voltage and practical capacity of various cathode materials presently used in LIBs are compared in Figure 1.

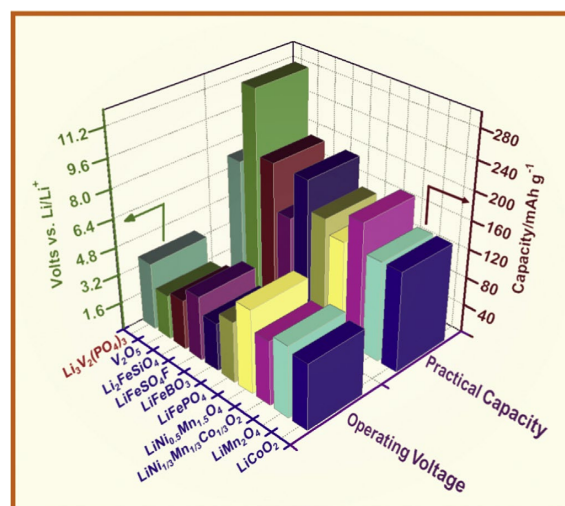


**Figure 1.** Comparison of operating voltage and practical capacity of various cathode materials presently used in lithium-ion batteries [9].

The purpose of this review is to report recent advancements in developing novel cathode materials as a possible replacement for layered lithium cobalt oxide in LIBs. In this review, three broad categories of cathode materials setting the pace for the next-generation LIBs are studied: (i) lithiated

transition metal oxides, (ii) vanadium pentoxides, and (iii) polyanion-type materials. An overview on the conventional LIB is also included in this review. Moreover, the various challenges hindering the full integration of these cathode materials in commercial LIBs and feasible solutions are accentuated in this study.

## 1.1 Conventional Li-ion battery

A typical LIB mainly consists of a negative electrode (anode), and a positive electrode (cathode) separated and connected by a  $\text{Li}^+$  conducting electrolyte, as described in Figure 2. The first-generation LIB employs the graphite as an anode, the layered  $\text{LiCoO}_2$  as a cathode, and the organic liquid of  $\text{LiPF}_6$ /ethylene carbonate (EC)/dimethylene carbonate as an electrolyte [9],[54]–[56]. During the electrochemical process of charging, lithium ions leave the  $\text{LiCoO}_2$  host structure and migrate through the electrolyte to the graphite, while the associated electrons are driven by an external power flow from the cathode to anode [9]. On discharging, Li ions and electrons move reversely. The LIB performance (e.g., cell potential, capacity, or energy density) is largely dependent on the intrinsic chemistry of negative and positive electrode materials [9]. The basic requirements for electrode material selection include [57]–[60]: (i) a high specific charge and charge density; (ii) a high (cathode) and low (anode) standard redox potential; (iii) electrochemical compatibility with the electrolyte solution; (iv) a facile electrode kinetic; (v) a high degree of reversibility; (vi) environmental benignity; (vii) safety; and (viii) moderate cost.

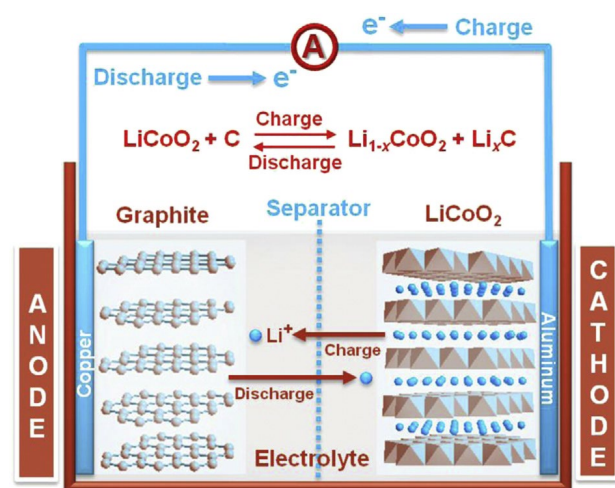


**Figure 2.** Schematic illustration of a lithium-ion battery employing graphite as anode and layered  $\text{LiCoO}_2$  as cathode [9].

Cathode materials are typically oxides of transition metals, which can undergo oxidation to higher valences when lithium is removed [61],[62]. While oxidation of the transition metal can maintain charge neutrality in the compound, large compositional changes often lead to phase changes. Thus, crystal structures that are stable over wide ranges of composition are recommended. Structural stability of the cathode material is a particular challenge during charging when most (ideally all) of the lithium is removed from the cathode [15]. During discharge lithium is inserted into the cathode material, and electrons from the anode reduce the

transition metal ions in the cathode to a lower valence. The rates of these two processes, as well as access of the lithium ions in the electrolyte to the electrode surface, control the maximum discharge current [15]. Exchange of lithium ions with the electrolyte occurs at the electrode-electrolyte interface [15]. Hence, cathode performance depends critically on the electrode microstructure and morphology, as well as the inherent electrochemical properties of the cathode material [15].

## 2. CATHODE MATERIALS

In recent years, a significant research effort has been devoted to developing high-performance cathode materials for next-generation LIBs in satisfying stringent requirements of electric vehicles and large-scale energy storage. Amongst them are lithiated transition metal oxides, vanadium pentoxides, and polyanion-type materials.

### 2.1 Lithiated transition metal oxides

The lithiated transition metal oxides as cathode materials for LIBs are reviewed under two main categories: lithium-rich layered oxides and nickel-rich layered oxides.

#### 2.1.1 Lithium-rich layered oxides

Among the prospective cathode materials for LIBs, lithium-rich layered oxide materials  $x\text{Li}_2\text{MnO}_3 \cdot (1-x)\text{LiMO}_2$  ( $M = \text{Mn}, \text{Ni}, \text{Co}, \text{Fe}, \text{Cr}, \text{etc.}$ ) have attracted much attention in recent years due to their large capacities ( $>280 \text{ mAhg}^{-1}$ ) with 3.6 V or larger operating voltages [63]. Some of the numerous challenges facing the utilization of these materials in commercial LIBs include low initial coulombic efficiency, poor rate capability, and voltage degradation during cycling [63]. However, in recent years, considerable progress has been reported in overcoming these challenges [63].

Layered-structure  $\text{LiNi}_{0.5}\text{Co}_{0.2}\text{Mn}_{0.3}\text{O}_2$  has been a promising cathode material for rechargeable lithium batteries due to their relatively low cost, less toxicity and high discharge capacity ( $>200 \text{ mAh g}^{-1}$ ) above a voltage of 4.5 V [63]. However, the large-scale application of  $\text{LiNi}_{0.5}\text{Co}_{0.2}\text{Mn}_{0.3}\text{O}_2$  cathode materials has been hindered by the severe capacity fading and poor rate performance at high voltage or high current density over numerous cycles [63]. One facile approach to combat these shortcomings is a surface modification using fluorides, phosphates, and metal oxides to suppress the side reactions and the phase transformation at the interface, thus slowing the capacity degradation and strengthening the structural stability [63]–[72]. Wang et al. [68] reported that zirconium doped  $\text{LiNi}_{0.5}\text{Co}_{0.2}\text{Mn}_{0.3}\text{O}_2$  materials were prepared by solid state method. The zirconium doping reduced the cation mixing degree and enlarged the interplanar spacing, which enabled the lithium ion to migrate easily in the crystal structure of the doped cathode materials. Hence, the zirconium doped samples,  $\text{Li}(\text{Ni}_{0.5}\text{Co}_{0.2}\text{Mn}_{0.3})_{0.99}\text{Zr}_{0.01}\text{O}_2$ , exhibited a capacity retention of 83.78% at 1 C after 100 repeated cycle in a high voltage of 4.6 V, while that of bare sample retained only 69.35%. Additionally, the rate capability of  $\text{Li}(\text{Ni}_{0.5}\text{Co}_{0.2}\text{Mn}_{0.3})_{0.99}\text{Zr}_{0.01}\text{O}_2$  was also significantly reinforced, especially at high current density. The improved electrochemical performances of the zirconium doped samples

were attributed to the less cation mixing degree, better lithium transportation kinetic, and lower impedance.

Niobium dopants have been reported as the most attractive candidates with the mutual effect of consolidating structure stability and boosting electrical conductivity of electrode materials for LIBs [73]–[77]. For instance, Wu et al. [78] synthesised Nb-doped  $\text{LiNi}_{1/3}\text{Co}_{1/3}\text{Mn}_{1/3}\text{O}_2$  with improved capacity retention, resulting from the more stable structure and lower resistance. Yang et al. [73] also investigated the effect of niobium (Nb) doping on the structure, and electrochemical performance of  $\text{LiNi}_{0.5}\text{Co}_{0.2}\text{Mn}_{0.3}\text{O}_2$  cathode materials for LIBs was reported. A controlled Nb doping strategy was adopted to conquer the drawbacks of  $\text{LiNi}_{0.5}\text{Co}_{0.2}\text{Mn}_{0.3}\text{O}_2$ , including the unstable structure and restricted lifespan. The spherical precursor  $\text{Ni}_{0.5}\text{Co}_{0.2}\text{Mn}_{0.3}(\text{OH})_2$  and  $\text{Li}(\text{Ni}_{0.5}\text{Co}_{0.2}\text{Mn}_{0.3})_{1-x}\text{Nb}_x\text{O}_2$  ( $x=0, 0.005, 0.01, 0.02$ ) were prepared by hydroxide co-precipitation and solid-state method. The  $\text{Li}^+/\text{Ni}^{2+}$  cation mixing degree was reduced with Nb doping. Besides, the rate capability and cycling stability of  $\text{LiNi}_{0.5}\text{Co}_{0.2}\text{Mn}_{0.3}\text{O}_2$  were improved by Nb doping. The experimental results showed that  $\text{Li}(\text{LiNi}_{0.5}\text{Co}_{0.2}\text{Mn}_{0.3})_{0.99}\text{Nb}_{0.01}\text{O}_2$  sample with appropriate Nb doping amount exhibited high capacity retention of 93.77% after 100 cycles at 1.0 C and enhanced rate performance with  $125.5 \text{ mAh g}^{-1}$  at 5.0 C, which is more superior to that of  $\text{LiNi}_{0.5}\text{Co}_{0.2}\text{Mn}_{0.3}\text{O}_2$  sample. Additionally, at elevated temperature ( $55^\circ\text{C}$ ), the Nb doping displayed further remarkable effect on stabilizing the structure, and 88.63% of the initial reversible capacity could be retained, which is  $\sim 20\%$  higher than that of the  $\text{LiNi}_{0.5}\text{Co}_{0.2}\text{Mn}_{0.3}\text{O}_2$ . Therefore, controlled Nb doping can improve the structural stability and electrochemical performance of advanced  $\text{LiNi}_{0.5}\text{Co}_{0.2}\text{Mn}_{0.3}\text{O}_2$  cathode materials to develop high energy density LIBs.

Zhou et al. [79] synthesised Sn-doped  $\text{Li}_{1.2}\text{Mn}_{0.54}\text{Ni}_{0.13}\text{Co}_{0.13}\text{O}_2$  cathode materials for LIBs with enhanced electrochemical performance using a sol-gel method. Doping with an appropriate amount of  $\text{Sn}^{4+}$ , the electrochemical performance of  $\text{Li}_{1.2}\text{Mn}_{0.54-x}\text{Ni}_{0.13}\text{Co}_{0.13}\text{Sn}_x\text{O}_2$  cathode materials was remarkably improved at  $x = 0.01$ . The substitution of  $\text{Sn}^{4+}$  for  $\text{Mn}^{4+}$  widens the  $\text{Li}^+$  diffusion channels owing to its larger ionic radius compared to  $\text{Mn}^{4+}$  and boosts the structural stability of Li-rich oxides, leading to an improved electrochemical performance in the Sn-doped  $\text{Li}_{1.2}\text{Mn}_{0.54}\text{Ni}_{0.13}\text{Co}_{0.13}\text{O}_2$  cathode materials. The  $\text{Li}_{1.2}\text{Mn}_{0.53}\text{Ni}_{0.13}\text{Co}_{0.13}\text{Sn}_{0.01}\text{O}_2$  electrode delivered a high initial discharge capacity of  $268.9 \text{ mAh g}^{-1}$  with an initial coulombic efficiency of 76.5% and a reversible capacity of  $199.8 \text{ mAh g}^{-1}$  at 0.1 C with capacity retention of 75.2% after 100 cycles. The rate performance of  $\text{Li}_{1.2}\text{Mn}_{0.54-x}\text{Ni}_{0.13}\text{Co}_{0.13}\text{Sn}_x\text{O}_2$  (LMNCS) electrodes compared to  $\text{Li}_{1.2}\text{Mn}_{0.54}\text{Ni}_{0.13}\text{Co}_{0.13}\text{O}_2$  (LMNC) electrodes between 2.0 and 4.8 V is illustrated in Figure 3a, while Figure 3b displays the variations of discharge capacities of the electrodes with discharge current density. The  $\text{Li}_{1.2}\text{Mn}_{0.53}\text{Ni}_{0.13}\text{Co}_{0.13}\text{Sn}_{0.01}\text{O}_2$  (LMNCS1) electrode exhibited the superior rate capability with discharge capacities of 239.8, 198.6, 164.4, 133.4, and  $88.8 \text{ mAh g}^{-1}$  at 0.2, 0.5, 1, 2, and 5 C, respectively, which are much higher than those of LMNC (196.2, 153.5, 117.5, 92.7, and  $43.8 \text{ mAh g}^{-1}$  at 0.2, 0.5, 1, 2, and 5 C, respectively) as shown in Figure 3. The excellent rate performance of the Sn-doped electrodes is attributed to the enlargement of  $\text{Li}^+$  diffusion channels caused by the doping of  $\text{Sn}^{4+}$ , which is favourable to the intercalation/deintercalation of  $\text{Li}^+$  [80],[81].

Besides, the discharge capacities for all electrodes decrease with the increasing discharge rate, as depicted in Figure 3b. This can be credited to the increased polarization at high rates [82].

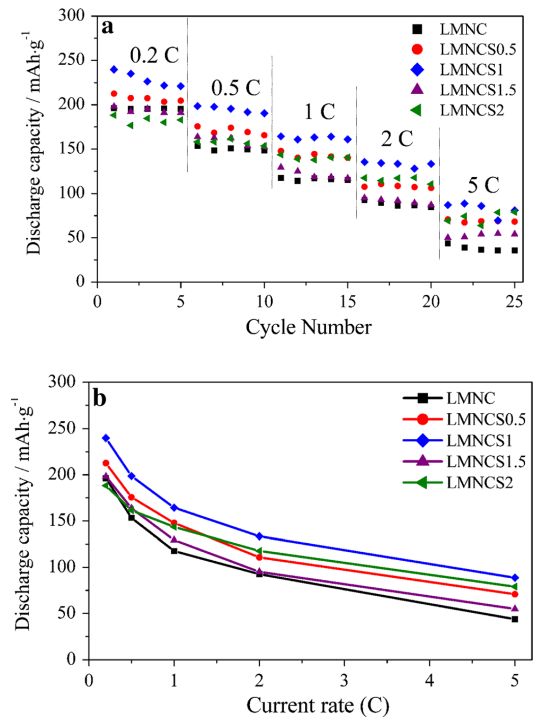


**Figure 3.** (a) Rate capability of the LMNC and LMNCS electrodes between 2.0 and 4.8 V; (b) Variations of the highest discharge capacity with discharge rate [79].

Furthermore, Yang et al. [83] demonstrated the use of  $\text{Li}_4\text{V}_2\text{Mn}(\text{PO}_4)_4$  (labelled as LVMP) in coating Li-rich Mn-based cathode materials ( $\text{Li}[\text{Li}_{0.2}\text{Mn}_{0.54}\text{Ni}_{0.13}\text{Co}_{0.13}]\text{O}_2$ ) (labelled as LNCMO) to reduce the residual Li compounds on the surface and prevent the dissolution of transition metals during cycling. LVMP is a composite cathode material with three-dimensional Li-ion diffusion channels and a stable structure at high operating voltages ( $> 4.5 \text{ V}$ ). In addition, it has been reported that LVMP has excellent electrochemical performance due to the “mutual doping” between  $\text{Li}_3\text{V}_2(\text{PO}_4)_3$  and  $\text{LiMnPO}_4$  [83]–[85]. Theoretical calculations proved that LVMP reduces the Li-ion diffusion energy barrier and provides efficient diffusion pathways to enhance the kinetic performance of the LNCMO. The as-synthesised LNCMO@LVMP compounds delivered a discharge capacity of  $300 \text{ mAh g}^{-1}$  with a high initial coulombic efficiency (84.2%) and excellent cycling stability (capacity retention of 82% after 50 cycles at 2C and 78.1% after 200 cycles at 1 C) coupled with a good rate performance ( $157.5 \text{ mAh g}^{-1}$  at 2 C). Therefore, the phosphate-based materials provide a new structural design strategy towards achieving excellent energy and power density in Li-rich materials.

Layered  $\text{LiNi}_{1-x-y}\text{Co}_x\text{Al}_y\text{O}_2$  (denoted as NCA,  $1-x-y>0.5$ ) materials have attracted great interest because of their encouraging features such as appealing capacity ( $>200 \text{ mAh g}^{-1}$ ), good cycling performance, and low cost of raw materials [86]–[90]. For instance,  $\text{LiNi}_{0.8}\text{Co}_{0.15}\text{Al}_{0.05}\text{O}_2$  has been recommended as cathode material of LIBs for electric vehicles in Tesla Model S due to its highly reversible capacity and modest cyclic stability as compared with  $\text{LiCoO}_2$  and  $\text{LiFePO}_4$

[91]– [93]. However,  $\text{LiNi}_{0.8}\text{Co}_{0.15}\text{Al}_{0.05}\text{O}_2$  still suffers from poor cycling stability and thermal instability during cycling. To overcome this shortcoming, LCNA materials with high capacity, excellent cycling life, and superior thermal stability have been exploited to deliver better performance for LIBs [86]. A practical approach for increasing the capacity of LNCA materials is by raising the electrochemically active Ni content as demonstrated for  $\text{LiNi}_{0.85}\text{Co}_{0.10}\text{Al}_{0.05}\text{O}_2$ , which delivered a higher capacity ( $233 \text{ mAh g}^{-1}$  at 0.1 C) than  $\text{LiNi}_{0.81}\text{Co}_{0.10}\text{Al}_{0.09}\text{O}_2$  ( $227 \text{ mAh g}^{-1}$ ) [88]. However, the  $\text{LiNi}_{0.85}\text{Co}_{0.10}\text{Al}_{0.05}\text{O}_2$  with higher Ni content exhibits severe cyclic deterioration and thermal instability compared to  $\text{LiNi}_{0.81}\text{Co}_{0.10}\text{Al}_{0.09}\text{O}_2$  [88],[94]. To mitigate the adverse effects of increased Ni content, Zhou et al. [86] proposed an easy co-precipitation synthesis of Ni-rich microspherical  $\text{Ni}_{0.9}\text{Co}_{0.07}\text{Al}_{0.03}(\text{OH})_2$  precursor with uniform particle size and large Brunauer-Emmett-Teller (BET) specific surface area of  $173.88 \text{ m}^2 \text{ g}^{-1}$  employing  $\text{AlO}_2^-$  as Al source. The co-precipitation technique combined the advantages of high tap density ( $>2 \text{ g cm}^{-3}$ ) with stable reactivity of microspheres and high activity with short paths for ion/electron diffusion of nanoparticles [86]. The uniform and dense  $\text{LiNi}_{0.9}\text{Co}_{0.07}\text{Al}_{0.03}\text{O}_2$  microspheres with well-assembled nanoparticles and a low degree of  $\text{Ni}^{2+}/\text{Li}^+$  mixing were synthesised by optimizing calcination conditions. The as-prepared  $\text{LiNi}_{0.9}\text{Co}_{0.07}\text{Al}_{0.03}\text{O}_2$  displayed a remarkable high initial reversible capacity of  $236 \text{ mA h g}^{-1}$  at 0.1 C and good cycling performance (with capacity retention of 93.1% after 100 cycles at 1 C and 86.3% after 200 cycles at 2 C). Additionally, the sample also demonstrated superior cyclic stability at elevated temperatures of 45, 55, and 60 °C. The experimental results obtained confirmed that  $\text{LiNi}_{0.9}\text{Co}_{0.07}\text{Al}_{0.03}\text{O}_2$  possessed good thermal stability (heat generation of  $517.5 \text{ J g}^{-1}$  at 4.3 V), fast lithium-ion diffusion ( $\sim 7 \times 10^{-10} \text{ cm}^2 \text{ s}^{-1}$ ), and high electronic conductivity ( $\sim 5.4 \times 10^{-4} \text{ S cm}^{-1}$ ). Moreover, the authors reported that the as-synthesised  $\text{LiNi}_{0.9}\text{Co}_{0.07}\text{Al}_{0.03}\text{O}_2$  exhibited superior capacity, better cycling performance, and higher rate capability than other reported Ni-based  $\text{LiNi}_{1-x}\text{U}_x\text{O}_2$  materials. The impressive electrochemical performance of the cathode material was attributed to the combination of the high Ni component, layered structure with a low degree of  $\text{Ni}^{2+}/\text{Li}^+$  mixing, and uniform microspheres with homogenous distribution of Ni, Co, and Al. Additionally, the assembled  $\text{LiNi}_{0.9}\text{Co}_{0.07}\text{Al}_{0.03}\text{O}_2/\text{KS}_6$  full cell delivered high capacities of 210 and  $180 \text{ mAhg}^{-1}$  at 0.1 and 1C, respectively, as depicted in Figure 4.

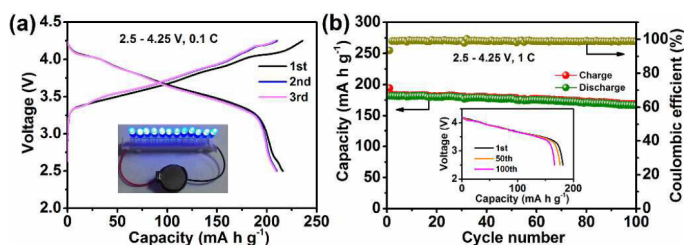


**Figure 4.** Electrochemical properties of  $\text{LiNi}_{0.9}\text{Co}_{0.07}\text{Al}_{0.03}\text{O}_2/\text{KS}_6$  full cell. (a) Charge and discharge profiles at selected cycles at a rate of 0.1 C. (b) Cycling performance at a rate of 1 C. Inset: discharge profiles at selected cycles [86].

The full cell also exhibited capacity retention of 91.7% after 100 cycles. Therefore, the as-prepared  $\text{LiNi}_{0.9}\text{Co}_{0.07}\text{Al}_{0.03}\text{O}_2$  is a potential candidate for cathode material of advanced LIBs owing to its prominent stable structure, excellent electrochemical performance, and thermal stability.

Wan et al. [95] reported the effects of Mn or Ti doping on the crystalline structure and electrochemical properties of NCA ( $\text{LiNi}_{0.85}\text{Co}_{0.10}\text{Al}_{0.05-x}\text{M}_x\text{O}_2$ ,  $\text{M}=\text{Mn}$  or  $\text{Ti}$ ,  $x < 0.01$ ) cathode materials. The NCA cathode material was prepared by one step of hydrothermal reaction at 170 °C and doped with either Mn or Ti since they have similar atomic radii as that of Ni and, in coordination with oxygen, can replace the transition metal atoms in the octahedral interstitial sites. This process can enhance thermal and structural stability and, in some cases, decrease electronic and ionic resistance [96],[97]. Mn and Ti doping resulted in cell volume expansion. This larger volume also improved the electrochemical properties of the cathode materials because  $\text{Mn}^{4+}$  and  $\text{Ti}^{4+}$  were introduced into the octahedral lattice space occupied by the Li-ions to expand the Li layer spacing and, thereby, improved the lithium diffusion kinetics. Consequently, the NCA-Ti electrode demonstrated superior performance with a high discharge capacity of  $179.6 \text{ mAh g}^{-1}$  after the first cycle, approximately  $23 \text{ mAh g}^{-1}$  higher than that obtained with the undoped NCA electrode, and  $166.7 \text{ mAh g}^{-1}$  after 30 cycles. A good coulombic efficiency of 88.6% for the NCA-Ti electrode was observed in the first charge and discharge capacities. Besides, the NCA-Ti cathode material displayed outstanding cycling stability of 93% up to 30 cycles.

### 2.1.2 Nickel-rich layered oxides

Ni-rich cathode materials  $\text{LiNi}_x\text{Co}_y\text{Mn}_z\text{O}_2$  ( $x+y+z=1$ ,  $x \geq 0.6$ ), labelled as Ni-rich NCM, have higher gravimetric energy density than  $\text{LiNi}_x\text{Co}_y\text{Mn}_z\text{O}_2$  ( $x+y+z=1$ ,  $x \leq 0.5$ ), which makes them one of the most promising cathode materials for high-energy LIBs [98],[99]. However, their structural and thermodynamic stability, cycle, and rate performances require further improvement before their full commercialisation as cathode materials in LIBs [100]. For instance, it is still a challenge to acquire stable high energy density from Ni-rich cathode materials under high operating voltage [101] because high operating voltages facilitate the dissolution of transition-metal ions into the electrolyte and damage the surface layered structure [102]. Besides, the structural transformation (layered  $\rightarrow$  spinel  $\rightarrow$  rock salt) of Ni-rich cathode materials at the surface is aggravated by the migration of  $\text{Ni}^{2+}$  ions with a low energy barrier into Li slabs owing to their similar ionic radius to  $\text{Li}^+$  [103],[104]. This surface phase transformation, together with the degree of  $\text{Li}^+/\text{Ni}^{2+}$  mixing is worsened by increasing the Ni content in  $\text{LiNi}_x\text{Co}_y\text{Mn}_z\text{O}_2$  cathode materials and especially under high operating voltage (4.5 V) [105]–[107]. In recent years, remarkable efforts have been focussed on improving the structural stability of Ni-rich materials by decreasing cationic mixing and inhibiting interfacial side reactions, such as lattice doping [108],[109] and surface reconstruction [110]–[113]. Specifically, lattice doping can stabilize the bulk structure, whereas surface modifications can reduce the side reactions on the electrode/electrolyte interface and inhibit the dissolution of transition metal ions. Wu et al. [98] demonstrated the use of rare earth element Ce (obtainable from the economically and environmentally friendly raw material, cerous nitrate) to reinforce the interface of Ni-rich

$\text{LiNi}_{0.8}\text{Co}_{0.1}\text{Mn}_{0.1}\text{O}_2$  cathode materials for LIBs under high operating voltage. The authors synthesised a series of modified samples through the reaction between cerous nitrate and  $\text{LiNi}_{0.8}\text{Co}_{0.1}\text{Mn}_{0.1}\text{O}_2$  at different calcination temperatures, as depicted in Figure 5. At the calcination temperature of above  $500\text{ }^\circ\text{C}$ , a  $\text{CeO}_2$  coating layer is formed to protect the electrode from erosion by the electrolyte and alleviate the increasing resistance during cycling [98],[114],[115]. During the calcination process,  $\text{Ce}^{4+}$  ions with strong oxidizing properties promote the oxidation of  $\text{Ni}^{2+}$  to  $\text{Ni}^{3+}$ , which effectively reduces the degree of  $\text{Li}^+/\text{Ni}^{2+}$  mixing in the surface lattice [116]. Additionally, the inert  $\text{Ce}^{3+}$  ions in transition metal slabs with strong Ce-O bonds help maintain the layered structure of Ni-rich cathode materials at high delithiation state [117]–[119]. Consequently, the modified Ni-rich materials fabricated with an erosion-resistant  $\text{CeO}_2$  layer outside and stronger Ce-O bonds inside with reduced  $\text{Li}^+/\text{Ni}^{2+}$  mixing exhibited excellent electrochemical properties, especially at high operating voltages. For example, the 50th capacity retention at  $0.2\text{ C}$  within  $2.75\text{--}4.5\text{ V}$  was improved from  $178.7\text{ mAhg}^{-1}$  (89.8%) to  $196.8\text{ mAhg}^{-1}$  (99.2%) after Ce salt modification at  $600\text{ }^\circ\text{C}$ .

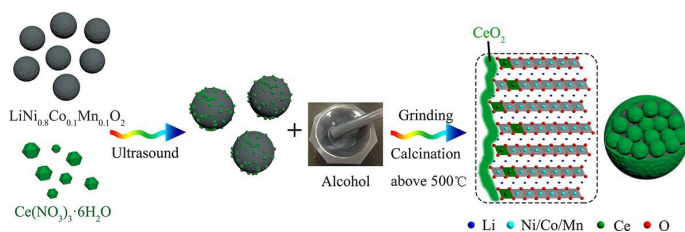


**Figure 5.** Schematic diagrams of the synthesis process and the structure of modified Ni-rich cathode materials with a  $\text{CeO}_2$  coating layer outside and  $\text{Ce}^{3+}$  doping inside [98].

However, it has been reported that the negative effect of residual lithium species on NCM can be overcome during manufacturing by coating the Ni-rich NCM with the  $\text{Li}_3\text{PO}_4$  protective layer to vastly enhance the cycling stability and rate capability of the cathode material [120],[122],[123]. Fan et al. [120] synthesised a unique synergistic multifunctional coating layer on the surface of  $\text{LiNi}_{0.8}\text{Co}_{0.1}\text{Mn}_{0.1}\text{O}_2$  (NCM811) by transforming the residual lithium species into  $\text{Li}_3\text{PO}_4$  and attaching graphene fragments. According to the microscopy studies performed by the authors, a  $10\text{ nm}$  amorphous  $\text{Li}_3\text{PO}_4$  layer together with nanosized  $\text{Li}_3\text{PO}_4$  particles uniformly covered the surface of NCM811 while the graphene fragments connected the NCM spherical particles to form electronic network. Owing to the synergistic effect of the  $\text{Li}_3\text{PO}_4$  (LPO) coating layer and the graphene network (GN), the modified sample (GN-LPO-NCM811) exhibited high-capacity retention of  $94.3\%$  after 150 cycles at  $0.5\text{ C}$  between  $3.0$  and  $4.3\text{ V}$ , while the pristine material displayed considerably lower retention of only  $88.1\%$ . Besides, the GN-LPO-NCM811 also demonstrated improved cycling stability at an elevated temperature of  $55\text{ }^\circ\text{C}$ ; the half-cell of GN-LPO-NCM811 achieved high-capacity retention of  $80\%$  after 400 cycles at  $20\text{ C}$ . As part of its outstanding electrochemical performance, the GN-LPO-NCM811 delivered  $70\%$  of its initial capacity at an extremely high rate of  $10\text{ C}$ , while the pristine NCM811 only supplied  $50\%$  of the capacity. The outcome of the EIS (electrochemical impedance spectrum) studies conducted by the authors confirmed that the  $\text{Li}_3\text{PO}_4$  apart from protecting

the materials from side reactions with the electrolytes also enhances the  $\text{Li}^+$  transportation at the electrode/electrolyte interface. Similarly, the electronic network bridged by graphene fragments provides fast electron transfer. Additionally, the thermal stability of the GN-LPO-NCM811 was significantly improved due to the protection from the mixed-conducting coating layer. The GN-LPO-NCM811 with high ionic conductivity and excellent electronic conductivity offers a template for engineering the surface of Ni-rich NCM cathode materials of the future [120].

To overcome some of the challenges responsible for poor electrochemistry performances of Ni-rich materials, Su et al. [124] designed and synthesised a structure-gradient  $\text{LiNi}_{0.8}\text{Co}_{0.1}\text{Mn}_{0.1}\text{O}_2$  (APS-NCM) cathode material with a high compaction density and superior rate performance using a secondary co-precipitation method. The structure comprised closely stacked nanoparticles as the core and directionally aligned nanosheets with exposed active planes as the shell. Besides, the structure-gradient design combined the advantages of high compacted density from the core and fast  $\text{Li}^+$  transport from the shell. Consequently, the APS-NCM possessed a high compaction density with excellent electrochemical performances, especially at high rates. APS-NCM delivered  $160\text{ mAh g}^{-1}$  discharge capacity even at  $10\text{ C}$ , while that of original  $\text{LiNi}_{0.8}\text{Co}_{0.1}\text{Mn}_{0.1}\text{O}_2$  material was only  $99.1\text{ mAh g}^{-1}$  within  $2.75\text{--}4.3\text{ V}$  (vs.  $\text{Li}^+/\text{Li}$ ). In addition, the 100th cycling capacity retention also increased from  $84.9\%$  to  $95.9\%$  at  $0.2\text{ C}$ . Although, the compaction density of APS-NCM decreased a little, its volumetric energy density was significantly improved. The proposed strategy for designing and synthesizing layered cathode materials with exposing  $\{010\}$  active planes and satisfied compaction density, can be developed further to meet different application requirements.

Moreover, Chen et al. [125] investigated the effect of dual-conductive layers on layered Ni-rich cathode material.  $\text{Li}_3\text{PO}_4$  combined with conducting polypyrrole (PPy) formed dual-conductive coating layers on  $\text{LiNi}_{0.8}\text{Co}_{0.1}\text{Mn}_{0.1}\text{O}_2$  cathode material to improve cycling and rate performance. These dual-conductive coating layers offered high ionic and electronic conductivity to the Ni-rich cathode materials. The  $\text{Li}_3\text{PO}_4$  coating layer remarkably improved the ionic conductivity of the cathode materials by removing the lithium residual on the particle surface and reducing the generation of HF in the electrolyte. On the other hand, the PPy layer prevents the direct contact between active cathode materials and electrolyte; thus, reducing the side reactions and dissolution of transition metals. Besides, the stretchy PPy capsule shell could reduce the generation of internal cracks by resisting the internal pressure. Therefore, the conductive PPy polymer enhanced the electrical conductivity of the cathode materials. The outcome of the electrochemistry tests revealed that the modified cathodes displayed much-improved cycling stability and rate capability. The modified cathode material retained  $95.1\%$  of its initial capacity at  $0.1\text{ C}$  after 50 cycles, while the bare sample retained only  $86\%$  and delivered  $159.7\text{ mAh g}^{-1}$  at  $10\text{C}$  compared with  $125.7\text{ mAh g}^{-1}$  for the bare sample. Hence, the dual-conductive coating layers composed of  $\text{Li}_3\text{PO}_4$  and PPy were very effective for improving the discharge capacity, rate capability, and capacity retention compared to raw or single coated Ni-rich cathode materials.

## 2.2 Vanadium pentoxide

Vanadium pentoxide ( $V_2O_5$ ), as a promising cathode material, has been intensively studied in LIBs for many years because of its natural abundance, low cost, typical layered crystal structure, good lithium-ion de-intercalation or intercalation properties, and high theoretical capacity of  $294 \text{ mAh g}^{-1}$  (corresponding to the insertion of two  $Li^+$  ions) [126]–[131]. However, the application of  $V_2O_5$  in LIBs is limited by poor diffusion coefficient, worse cycle stability, and low electronic conductivity [132]. Construction of nanostructure and preparation of carbon- $V_2O_5$  composite materials are generally considered as two practical approaches to shorten the transfer path for electrons and ions and to increase the electrode conductivity, respectively [133]–[136].

### 2.2.1 Micro- and nano-structured vanadium pentoxide

Several  $V_2O_5$ -based nanostructures such as nanowire [137]–[139], nanobelt [133],[140],[141] nanosheet [142]–[144], hollow nanosphere [145]–[148] and nanoflower [149] have been synthesised to improve the electrochemical performances of  $V_2O_5$ -based electrodes. Ramasami et al. [139] synthesised  $V_2O_5$  nanowire clusters ( $V_2O_5$ NWC) for applications in LIBs by a gel-combustion method using bio-fuel cassava starch (*Manihot esculenta*). The  $V_2O_5$ NWC exhibited a discharge capacity of  $188 \text{ mAh g}^{-1}$  with better capacity retention of 90% at the end of the 50th cycle, corresponding to a coulombic efficiency of about 99%. The scanning electron microscopic (SEM) images of  $V_2O_5$ NWC revealed both nanorod and nanowire morphologies which contributed to the good rate capability and cycling stability of the nanostructure.

Wu et al. [133] examined hierarchical sisal-like  $V_2O_5$  microstructures consisting of primary one-dimension (1D) nanobelt with [001] facets orientation growth and rich oxygen vacancies as cathode materials for LIBs. The microstructures were synthesised through a facile hydrothermal process using polyoxyethylene-20-cetyl-ether as a surface control agent and followed by calcination. The sisal-like  $V_2O_5$  delivered excellent electrochemical properties, including a longer cycling lifespan, higher reversible capacity, and higher rate capability. The as-synthesised microstructures benefitted from the synergistic effects of the primary 1D nanobelt and the stable [001] facets. The primary 1D nanobelt shortens the transfer path of electrons and ions, while the stable [001] facets could reduce the side reaction at the interface of electrode/electrolyte [133],[140]. Besides, the 1D nanobelts structure also alleviates the strain of volume expansion and offers excellent electronic conductivity along the longitudinal direction [133]. Moreover, the oxygen vacancies generated by the low valence state vanadium can facilitate the diffusion of lithium ions, thereby enhancing the conductivity and cycling stability of the  $V_2O_5$ -based materials [133]. The experimental results revealed that the sisal-like  $V_2O_5$  exhibited markedly higher rate performance than the bulk  $V_2O_5$  counterpart, which was synthesised by direct pyrolysis of  $NH_4VO_3$  under the same sintering processes. The sisal-like  $V_2O_5$  delivered the stable discharge capacities of 297, 261, 235, 211, 190, 160 and  $105 \text{ mAh g}^{-1}$  at 0.1, 0.2, 0.5, 1, 2, 5, 10 C (1 C =  $300 \text{ mA g}^{-1}$ ), respectively. However, the corresponding capacity of bulk  $V_2O_5$  was only 269, 244, 225, 175, 143, 92, and  $38 \text{ mAh g}^{-1}$ , respectively. With a remarkably high discharge capacity of  $297 \text{ mAh g}^{-1}$  at 0.1 C and excellent cycling stability, the sisal-

like  $V_2O_5$  microstructures are top candidates for advanced cathode materials for LIBs.

Porous hollow  $V_2O_5$  nanotubes (VNTs), apart from possessing the advantages of 1D nanostructure, also offer pores with different aperture and hollow structures [150]. Some of the merits of 1D nanostructure include shortened  $Li^+$  diffusion pathway, increased contact area between the active material and the electrolyte, the reduced charge transfer resistance, and the structural stability, which could improve the strain relaxation to withstand the volume expansion during  $Li^+$  insertion/extraction process [150]. Hence, VNTs as cathode materials for LIBs can improve the penetration of electrolytes, increase the contact surface area between the electrolyte and active material and accommodate the volume variations via additional void space during cycling [150]. Liu et al. [150] fabricated VNTs using electrospinning and successive sintering process. By controlling the calcination time, the cathode materials comprising  $V_2O_5$  were synthesised with good electrochemical performance and nanotubes morphology after sintering at  $400^\circ\text{C}$  for 2 hours in the air. The optimized VNTs electrode displayed enhanced electrochemical performance with good specific discharge capacities, cycling durability (capacity retaining 72.5% at 100 cycles), and improved high-rate performance ( $186 \text{ mAh g}^{-1}$  at  $1000 \text{ mA g}^{-1}$ ). This can be ascribed to the superior nanostructure with pores and hollow morphology.

Jiang et al. [151] reported a structural design and engineering of 1-D rod-like  $V_2O_5$  cathode materials for LIBs using polyphenol-grafted collagen fiber CF as a unique bio-temple. The collagen fiber was modified by bayberry tannin, a natural plant polyphenol, to enhance its affinity for vanadium anions. After simple calcination in air, the organic CF template was removed entirely, and simultaneously the rod-like  $V_2O_5$  was prepared. The as-prepared 1D rod-like  $V_2O_5$  displayed enhanced electrochemical performance as cathode materials for LIBs due to its unique structural merits. The SEM images of the natural collagen fiber and  $V_2O_5$  synthesised at a different temperature ranging from  $450$ – $650^\circ\text{C}$  are presented in Figure 6.

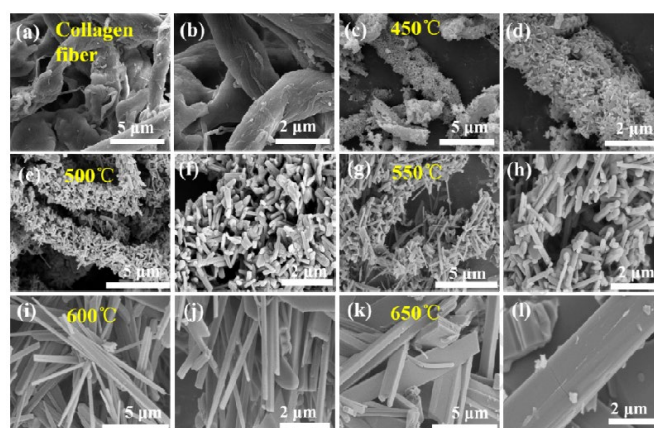


**Figure 6.** SEM images of natural CF (a-b) and 1D rod-like  $V_2O_5$  synthesised at different temperature ranging from  $450$ – $650^\circ\text{C}$  (c-l) [151].

Like the natural CF (Figure 6a-b), the  $V_2O_5$ -450 (i.e.,  $V_2O_5$  prepared at  $450^\circ\text{C}$ ) retain 1D ordered morphology of fibrous bundles, which comprise numerous  $V_2O_5$  particles (Figure 6c-f). However, those samples prepared at high temperatures over

500 °C show quite different morphology, which was constructed by the assemblage of primary  $V_2O_5$  crystals to form a long-rod-like architecture (Figure 6g-l). This phenomenon could be attributed to the crystal growth of  $V_2O_5$  along the direction of [001] during the annealing process above 500 °C. Amongst them, the  $V_2O_5$ -600 exhibits a relatively well-crystallized structure and uniform morphology than other samples [151]. Moreover, the transfer pathway of electrons and ions was shortened by the novel 1D rod-like structure. Also, the lithium-ion diffusion was enhanced by the oxygen vacancies generated by low valence state vanadium ( $V^{4+}$ ). Consequently, the 1D rod-like  $V_2O_5$  delivered a high specific capacity of 255 mAh  $g^{-1}$  at 0.1 C, and excellent rate capability of 100 mAh  $g^{-1}$  at 10 C. The method adopted by the authors provides a new strategy for the environmentally friendly and size-controlled synthesis of 1D rod-like  $V_2O_5$ -based cathode for efficient lithium storage.

## 2.2.2 Vanadium pentoxides carbon composite

Hydrated vanadium pentoxide ( $V_2O_5 \cdot nH_2O$ ) compared with crystalline  $V_2O_5$  exhibits better chemical stability and can reversibly absorb more than two lithium ions due to its enlarged interlayer spacing [126]. However, the exploration of  $V_2O_5 \cdot nH_2O$  cathode is limited by its inherently low conductivity and slow electrochemical kinetics, leading to a significant decrease in capability [126]. Several attempts have been made to improve the electrical conductivity and rate performance of  $V_2O_5 \cdot nH_2O$  cathode by incorporating carbon materials such as graphene [129],[152],[153], graphene oxide (GO) [129],[154], and carbon nanotubes (CNTs) [155]–157], into the cathode material owing to their extensive distribution, low density, high specific surface area, excellent electrical and thermal conductivity, mechanical stability, and environmentally friendly components [158]. Apart from effectively facilitating the charge transport, the insertion of carbon materials also accommodates the volume change caused by the intercalation and de-intercalation of lithium ions [126]. Although significant improvement in rate performance and electrical conductivity has been reported [159],[160], this was often achieved at the cost of a large amount of carbon coating (from 20 wt.% to 60 wt.%). The negative implication of the excessive amount of carbon materials is the consumption of lithium ions, which can affect cathode materials' capacity and even narrow the voltage window [126]. Therefore, research effort is being focussed on exploring the  $V_2O_5 \cdot nH_2O$ /carbon composite containing low carbon content without damaging the capability of LIBs. Zhang et al. [126] fabricated a crystalline  $V_2O_5 \cdot nH_2O$  nanobelts/reduced graphene oxide (rGO) composite with 8 wt.% carbon using a simple but effective dual electrostatic assembly strategy. The  $V_2O_5 \cdot nH_2O$ /rGO cathode material for LIBs displayed a high reversible capacity of 268 mAh  $g^{-1}$  at 100 mA  $g^{-1}$  and especially an excellent rate capability (196 mAh  $g^{-1}$  at 1000 mA  $g^{-1}$  and 129 mAh  $g^{-1}$  at 2000 mA  $g^{-1}$ ), surpassing those of the  $V_2O_5$ /carbon composites reported in the literatures [159],[160]. The outstanding performance of  $V_2O_5 \cdot nH_2O$ /rGO is attributed to the synergetic effects between one-dimensional  $V_2O_5 \cdot nH_2O$  nanobelts and two-dimensional rGO nanosheets, which provide a short transport pathway and enhanced electrical conductivity.

Furthermore, hierarchical nanoarchitecture has been proven to be highly effective in expanding accessible active sites and

providing a fast ion diffusion pathway in energy storage materials [161],[162]. Nak et al. [163] demonstrated the construction of a hierarchically open-porous  $V_2O_5$ /rGO composite microball for high-performance LIB cathodes using spray frozen technique combined with thermal reduction process. The open-porous surface of rGO microballs offers the advantages of immobilizing  $V_2O_5$  particles, enhancing the electronic conductivity, and stabilizing active  $V_2O_5$  crystals [163]. The radial orientation of the composite microballs effectively provides a fast diffusion pathway for Li-ion. Besides,  $V_2O_5$ /rGO composite microballs delivered initial discharge capacity of 273 mAh  $g^{-1}$  at 100 mA  $g^{-1}$ , which is greater than those of rGO (78 mAh  $g^{-1}$ ) and  $V_2O_5$  particles (214 mAh  $g^{-1}$ ). Additionally, the composite microballs displayed a better rate capability of 51.3% (compared to 36.4% for  $V_2O_5$  particles) and the capacity retention of 80.4% (two times greater than  $V_2O_5$  particles) Coulombic efficiency of 97.1% over 200 cycles, depicting enhanced cyclic stability. Hence, the unique composite microstructure architecture offers an excellent chemical approach to enhance the electrochemical performance of cathode materials for LIBs.

Various attempts have been made by researchers to synthesise porous carbon-based on natural porous structures of plants for the growth of  $V_2O_5$  nanostructure arrays. However, most of the achieved carbons have irregular microporous structures and rough surfaces, such as bamboo [164],[165], wood [166],[167], and lotus seed-pod shells [168], which are not suitable for the growth of  $V_2O_5$  nanostructures arrays inside them. In combating this challenge, Tan et al. [169] fabricated carambola-like  $V_2O_5$  nanoflowers arrays on the surface of natural microporous reed carbon (PRC) through a convenient high temperature carbonization process and hydrothermal method. The natural oxygen-containing groups formed on the carbon surface permit the direct growth of  $V_2O_5$  nanoflowers arrays on the PRC surface after a one-step hydrothermal process [169]. Owing to the novel composite structures, the as-prepared cathode material delivered an excellent discharge capacity of 273 mAh  $g^{-1}$  at 0.2 C after 100 cycles and significant capacity retention of 96.2%. The discharged capacity decreased to 180 mAh  $g^{-1}$  after 500 cycles at 2.0 C, with a capacity decay of 0.025% per cycle, and the average Coulombic efficiency of the battery was about 100% throughout the long-term cycles. Therefore, the as-synthesised  $V_2O_5$  nanoflowers arrays on PRC have demonstrated high-rate capability and excellent cycling stability, thereby qualifying them as high-performance cathode materials for LIBs.

Liang et al. [170] reported  $V_2O_5$ /CNTs composites prepared through a facile hydrothermal method. The composites as cathode materials for lithium-ion batteries exhibited improved electrochemical performance compared to electrode materials free of CNTs. The cycling performance of the  $V_2O_5$ /CNTs composites at a current density of 100 mA  $g^{-1}$  between 2–4 V is shown in Figure 7a. The  $V_2O_5$ -60CNT composites (containing 60-mg functional CNTs) delivered a high initial capacity of 305 mA h  $g^{-1}$ , and an excellent discharge capacity of 196.8 mA h  $g^{-1}$  at a current density of 100 mA  $g^{-1}$  after 50 cycles. However, the electrode materials free of CNTs ( $V_2O_5$ ) delivered an initial capacity of 263 mA h  $g^{-1}$ , and a discharge capacity of 171 mA h  $g^{-1}$  at a current density of 100 mA  $g^{-1}$  after 50 cycles (Figure 7a). The rate capability of  $V_2O_5$ /CNTs composites at various current densities within the potential window of 2–4V is depicted in Figure 7b.  $V_2O_5$ -60CNT displayed a higher discharge capacity (69.5 mA h  $g^{-1}$ ) than

$V_2O_5$  ( $55 \text{ mA h g}^{-1}$ ) at a rate of  $10 \text{ C}$  ( $1000 \text{ mA g}^{-1}$ ). After the high-rate cycling,  $V_2O_5$ -60CNT electrode delivered a discharge capacity of  $236 \text{ mAh g}^{-1}$  when the current density was returned to  $1 \text{ C}$  ( $100 \text{ mA g}^{-1}$ ).  $V_2O_5$ -30CNT (containing 30-mg functional CNTs) and  $V_2O_5$  delivered capacities of 195 and  $156 \text{ mAh g}^{-1}$  under the same conditions, respectively. Thus, the  $V_2O_5$ -60CNT electrode exhibited outstanding rate capability and capacity performance. The enhanced electrochemical performance can be attributed to the fact that the CNTs in the  $V_2O_5$ /CNTs composites can effectively facilitate ionic diffusion by raising the electrical conductivity.

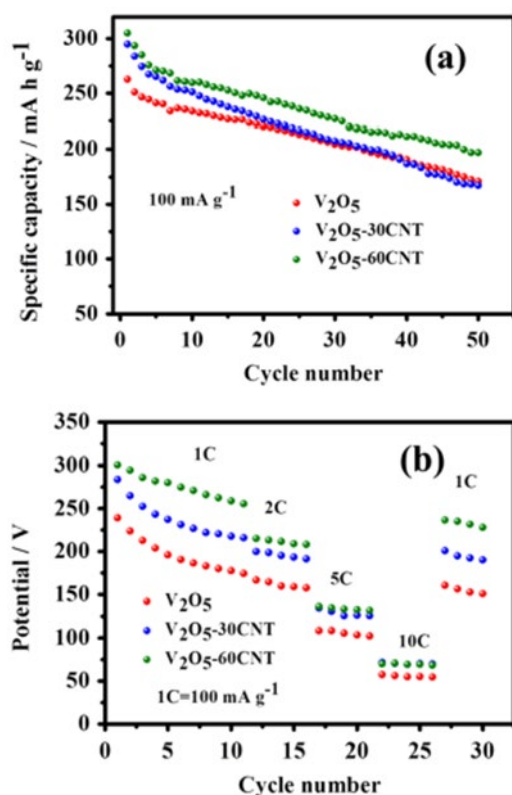


**Figure 7.** (a) Cycling performance of  $V_2O_5$ ,  $V_2O_5$ -30CNT, and  $V_2O_5$ -60CNT at a current density of  $100 \text{ mA g}^{-1}$ ; (b) rate capability of  $V_2O_5$ ,  $V_2O_5$ -30CNT, and  $V_2O_5$ -60CNT at different current densities [170].

### 2.2.3 Doped vanadium pentoxide thin film

Most of the methods proposed for improving the electrochemical performance of  $V_2O_5$  are usually time-consuming and expensive owing to the demands for the synthesis of complex process [171]. A facile and rational synthetic approach is the doping of  $V_2O_5$  with transition metal ions since the electronic conductivity and cycle stability can be increased by one order of magnitude compared with undoped cathode materials. Hu et al. [172] reported a porous Cu-doped  $V_2O_5 \cdot nH_2O$  thin film electrode, directly synthesised via low-temperature annealing and simple drop-casting method from  $V_2O_5/H_2O_2$  sol with various concentration copper ion ( $Cu^{2+}$ ). The experimental results confirmed that the mass fraction of  $Cu^{2+}$  influenced the morphologies, valence state of vanadium, and the electrochemical performance of Cu-doped  $V_2O_5 \cdot nH_2O$  thin film. For instance, when the mass fraction of  $Cu^{2+}$  was 1 wt.%, the prepared Cu-doped  $V_2O_5 \cdot nH_2O$  thin film electrode displayed porous network

nanostructure (Figure 8b) in contrast to the homogeneous smooth and dense surface of pure  $V_2O_5 \cdot nH_2O$  film (Figure 8a). Thus, 1 wt.% Cu-doped  $V_2O_5 \cdot nH_2O$  thin films displayed greater lithium-ion diffusion coefficients, better cycling stability, excellent electrochemical reversibility, and higher specific capacity than the pure  $V_2O_5 \cdot nH_2O$  thin film [172]. The Cu-doped  $V_2O_5 \cdot nH_2O$  thin film cathode delivered a high discharge specific capacity of  $344 \text{ mAh g}^{-1}$  at a current density of  $250 \text{ mA g}^{-1}$ . Excellent cycling stability with only 0.14% per cycle degradation during 104 cycles was obtained even at a high current density of  $550 \text{ mA g}^{-1}$ . Hence, 1 wt.% Cu-doped  $V_2O_5 \cdot nH_2O$  thin films hold great potentials as future cathode material for high-performance LIBs.

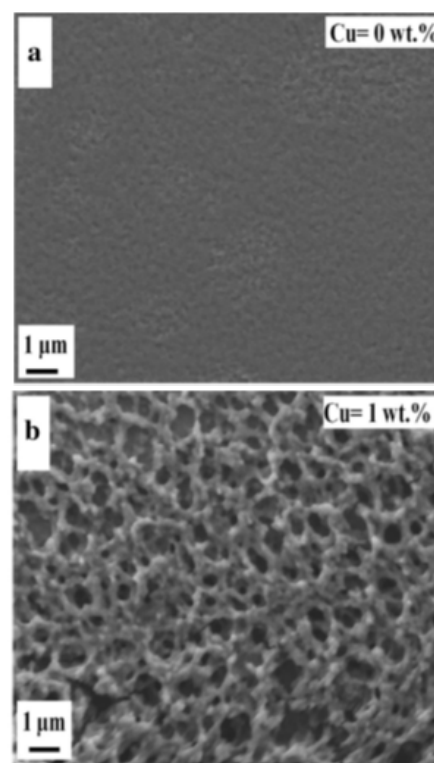


**Figure 8.** (a) SEM images of pure  $V_2O_5 \cdot nH_2O$  ( $Cu = 0 \text{ wt.}\%$ ) and (b) Cu-doped  $V_2O_5 \cdot nH_2O$  ( $Cu = 1 \text{ wt.}\%$ ) thin films [172].

### 2.3 Polyanion-type materials

Several researchers have investigated the positive effects of polyanion doping in improving the electrochemical performance and cycling stability of Ni-rich layered  $LiNi_{1-x-y}Co_xMn_yO_2$  cathode materials for LIBs. Generally, ion doping reduces cation mixing and widens the spacing between the lithium and transition metal layers to enhance the electrochemical performance [173]–[175]. In addition, polyanions consist of tetrahedral or octahedral anionic units, which stabilise the crystal structure [176]. For instance, Zhao et al. [177] reported that the gradient polyanion phosphorus doping into  $Li_{1.17}Mn_{0.5}Ni_{0.17}Co_{0.16}O_2$  enhanced the discharge capacity and cycling stability of the cathode material. The improved electrochemical performance of the doped cathode material can be attributed to the polyanion dopants which stabilised the oxygen close-packed structure and protected the cathode material from corrosion induced by electrolytes [177]. Similarly, Ma et al. [176] proposed that the excellent cycling

performance and structural stability are improved by  $\text{BO}_3^{3-}$  substitution for O in the  $\text{Li}_{1.16}(\text{Ni}_{0.25}\text{Mn}_{0.75})_{0.84}\text{O}_2$  system. Moreover, Zhang et al. [178] modified  $\text{LiNi}_{0.6}\text{Co}_{0.2}\text{Mn}_{0.2}\text{O}_2$  (NCM) cathode materials by substituting the boracic polyanion to suppress capacity degradation and enhance power performance. The boracic polyanion-doped samples possessed outstanding electrochemical performance, high lithium-ion diffusion coefficient rate, and small charge transfer impedance due to the stabilisation of the crystal structure by the boracic polyanion [178]. The modified NCM cathode materials exhibited superior rate property at high current density ( $131.02 \text{ mAh g}^{-1}$  at 5 C) compared to the bare NCM ( $115.96 \text{ mAh g}^{-1}$  at 5 C) and higher capacity retention (76.07% after 100 cycles at 1 C) than the bare NCM (59.15% after 100 cycles at 1 C). Also, the cation mixing declined from 4.65% to 3.21%. Therefore, the boracic polyanion doping can significantly improve the rate capabilities and cycling stability of the NCM cathode materials [178].

Xie et al. [179] synthesised and characterised boron-based polyanion-tuned ultrahigh-Ni layered cathodes (Ni content > 90%) for high-energy-density LIBs. The modified cathode materials  $\text{B}_2\text{O}_3\text{-LiNi}_{0.94}\text{Co}_{0.06}\text{O}_2$  (B-NC) delivered a discharge capacity of  $223 \text{ mAh g}^{-1}$  at C/3 with 80% capacity retention after 400 cycles in full cells with graphite anodes, superior to 61% retention for the bare  $\text{LiNi}_{0.94}\text{Co}_{0.06}\text{O}_2$  (NC). The improved cyclability was credited to the development of a well-passivated boron/phosphorus-rich cathode-electrolyte interphase in B-NC. Besides, B-NC exhibited a markedly enhanced air exposure and thermal stability owing to the presence of the doped boron polyanion (atomic boron) in its lattice structure which advances the oxygen structure stability. A 30-day air-stored B-NC delivered a discharge capacity of  $125 \text{ mA h g}^{-1}$  at 10 C rate, in sharp contrast to  $65 \text{ mA h g}^{-1}$  for the stored NC.

Even though polyanion electrode materials are superior in thermal and structural stability compared to layered basic oxides such as  $\text{LiCoO}_2$ ,  $\text{Li}(\text{Ni},\text{Mn},\text{Co})\text{O}_2$  and  $\text{Li}(\text{Ni},\text{Co},\text{Al})\text{O}_2$ , their commercialisation is seriously hampered by the low energy density. To overcome this shortcoming, Kim et al. [180] synthesised a novel Li-rich fluorophosphate compound,  $\text{Li}_5\text{V}_2\text{PO}_4\text{F}_8$ , capable of delivering high energy density that originated from both multi-electron reactions of vanadium and the high voltage induced by fluorine. The novel cathode material possessed a new crystal structure comprising a robust 3-D framework of corner-sharing octahedra  $\text{VO}_2\text{F}_4$  with tetrahedra  $\text{PO}_4$  and 3-D Li-ion diffusion pathways can facilitate the (de)intercalation of Li ions. The outcome of the electrochemical test showed that the as-prepared cathode material delivered the highest redox voltage,  $\sim 4.4 \text{ V}$  (vs.  $\text{Li}/\text{Li}^+$ ), among  $\text{V}^{3+}/\text{V}^{4+}$  redox reactions with  $111 \text{ mAh g}^{-1}$  of reversible capacity. During the first charge only, the cathode displayed an active redox reaction of the  $\text{V}^{4+}/\text{V}^{5+}$  at  $\sim 4.9 \text{ V}$  (vs.  $\text{Li}/\text{Li}^+$ ) with  $228 \text{ mAh g}^{-1}$  of charge capacity. Also, stable capacity retention and good rate capability at both charging and discharging rates up to 2 C rate were observed during the vanadium deficient phase. In addition, vanadium deficient  $\text{Li}_5\text{V}_2\text{PO}_4\text{F}_8$  phase exhibited stable capacity retention for 100 cycles at 1 C and fast rate capability of both charging and discharging at 2 C. Thus, the new Li-rich polyanion material,  $\text{Li}_5\text{V}_2\text{PO}_4\text{F}_8$  with high voltage and high energy density, is a very promising cathode for LIBs, and further investigation on chemical substitution would undoubtedly enhance its electrochemical performance.

Furthermore, Qiu et al. [181] demonstrated the co-doping of  $\text{PO}_4^{3-}$  polyanion and  $\text{Mn}^{4+}$  cation into Ni-rich  $\text{LiNi}_{0.80}\text{Co}_{0.15}\text{Al}_{0.05}\text{O}_2$  cathode in enhancing the structural stability and electrochemical performance of the cathode material for LIBs. The  $\text{Mn}^{4+}$  cation and  $\text{PO}_4^{3-}$  polyanion co-doped Ni-rich  $\text{LiNi}_{0.80}\text{Co}_{0.15}\text{Al}_{0.05}\text{O}_2$  cathode materials were synthesised by high-temperature solid-phase reaction using  $\text{Ni}_{0.80}\text{Co}_{0.15}\text{Al}_{0.05}(\text{OH})_2$  precursor and dopants (Figure 9). The modified materials offered reduced  $\text{Li}^+/\text{Ni}^{2+}$  cationic mixing, expanded thickness of lithium layered interslab, suppressed structural degradation, enhanced electrochemical reaction kinetic and cycling stability than the pristine cathode. In the cell potential of 2.7 – 4.3 V, the 3%  $\text{PO}_4^{3-}$  and  $\text{Mn}^{4+}$  co-doped cathode delivered a reversible discharge capacity of  $204 \text{ mAh g}^{-1}$  at 0.1 C, outstanding cycling stability with a capacity of  $174 \text{ mAh g}^{-1}$  and capacity retention of 85.5% at 1 C after 100 cycles, especially, and a superior discharge capacity of  $157.8 \text{ mAh g}^{-1}$  at 5 C. Even at an elevated temperature of  $55^\circ\text{C}$ , the cathode retained 80.9% of initial capacity ( $195 \text{ mAh g}^{-1}$ ) at 1 C after 100 cycles. Therefore, owing to the stabilisation role of  $\text{Mn}^{4+}$  and  $\text{PO}_4^{3-}$ , the modified materials with a moderate number of dopants possessed improved structural stability coupled with enhanced electrochemical performance, especially at elevated temperature and high cut-off cell potential. Moreover, the authors' polyanion and cation co-doping strategy serves as a template for the modification of Ni-rich layered oxides cathode materials.

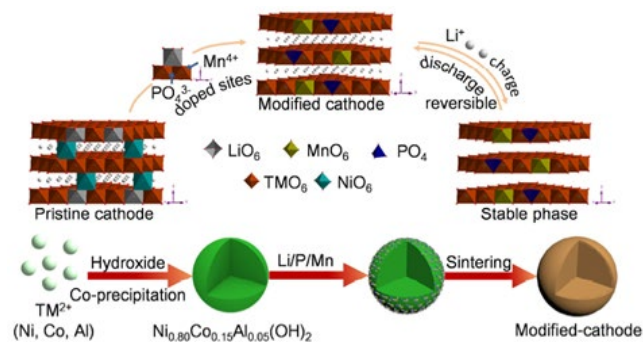


**Figure 9.** The schematic illustration for the synthesis of modified material and the corresponding crystal structure [181].

Compared with layered oxides, polyanionic compounds can provide longer cycling life and greater safety due to their stable polyanionic frameworks, characteristics that have helped olivine  $\text{LiFePO}_4$  secure great success in the market [182],[183]. However, the lower capacity arising from heavier and larger polyanionic groups is a disadvantage to their use. Therefore, anion engineering is considered essential for designing polyanionic compounds with improved cathode performance. Lu et al. [183] adopted a polyanion substitution strategy to explore a new series of polyanionic solid-solution alluaudite-type cathode materials,  $\text{Na}_x\text{Fe}_y(\text{PO}_4)_{3-z}(\text{SO}_4)_z$  ( $0 \leq z \leq 3$ ), that might exhibit enhanced electrochemical properties. The electrode properties of  $\text{Na}_x\text{Fe}_y(\text{PO}_4)_{3-z}(\text{SO}_4)_z$  ( $z = 0, 1, 1.5, 2, 3$ ) were measured at a C/50 current rate in the voltage range 2.0 – 4.5 V. The discharge capacity profiles of the polyanionic solid-solution cathodes are shown in Figure 10a. The phosphate  $\text{Na}_2\text{Fe}_3(\text{PO}_4)_3$  delivered a reversible capacity of approximately  $80 \text{ mAh g}^{-1}$  at a current rate of C/50 while the

voltage profile displays several distinct voltage plateaus. However, the voltage profiles become smooth, slopy curves after the substitution of polyanion  $\text{SO}_4$  into the structure, signifying single-phase reaction mechanisms. Interestingly, the average voltage increased markedly from 3.19 ( $z = 0$ ) to 3.36 ( $z = 1.5$ ) and, finally, to 3.72 V ( $z = 3$ ) by  $\text{SO}_4$  substitution as illustrated in Figure 10b. The elevated voltage is attributed to the inductive effect of the highly electronegative  $\text{SO}_4$  polyanion [183],[184]. Moreover, superior capacity can be acquired by the polyanionic solid-solution system after mixing two polyanions ( $\text{PO}_4$  and  $\text{SO}_4$ ) in the structure. For instance,  $\text{Na}_x\text{Fe}_y(\text{PO}_4)_{3-z}(\text{SO}_4)_z$  with  $z = 1.5$  ( $\text{Na}/\text{Fe} = 1$ ), delivered a larger reversible capacity ( $113.2 \text{ mAh g}^{-1}$ ) than the two end-members:  $\text{Na}_2\text{Fe}_3(\text{PO}_4)_3$  with  $z = 0$  ( $82.1 \text{ mAh g}^{-1}$ ) or  $\text{Na}_{2.56}\text{Fe}_{1.72}(\text{SO}_4)_3$  with  $z = 3$  ( $102.9 \text{ mAh g}^{-1}$ ) as depicted in Figure 10c. The poor measured capacity exhibited by  $\text{Na}_2\text{Fe}_3(\text{PO}_4)_3$ , extremely lower than its theoretical capacity of  $107.4 \text{ mAh g}^{-1}$ , may be ascribed to its larger particle size ( $0.5 - 2 \text{ }\mu\text{m}$ ) as compared with that (below  $200 \text{ nm}$ ) of the sulphate end member with  $z = 3$ , where phosphates tend to crystallise more facily than sulphates under the identical synthetic conditions. Additionally, the as-synthesised cathode materials exhibited tunable voltage and superior capacities depending on the mixing ratio of the two polyanions. The polyanion substitution strategy reported by the authors can contribute immensely to the development of new cathode materials for both Li-ion and Na-ion batteries.

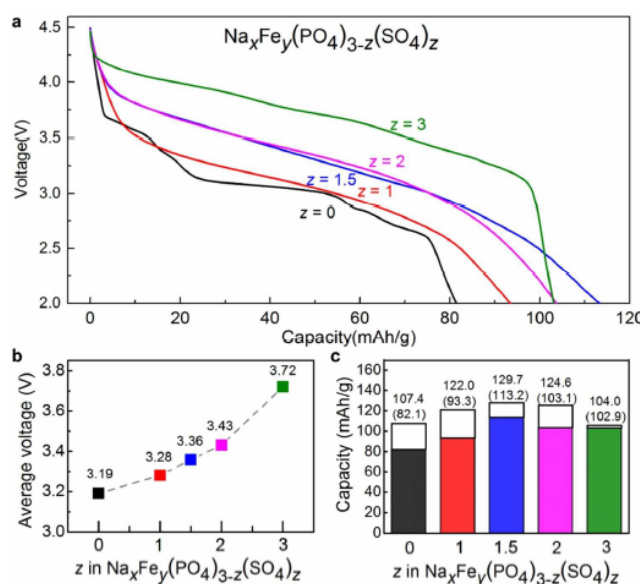


**Figure 10.** Electrochemical performance of  $\text{Na}_x\text{Fe}_y(\text{PO}_4)_{3-z}(\text{SO}_4)_z$  ( $z = 0, 1, 1.5, 2, 3$ ). (a) Discharging profiles cycled between 2.0–4.5 V at current rate C/50. (b) Variance of average discharging voltages. (c) Variance of theoretical and reversible capacities during  $\text{SO}_4$  substitution. Coloured areas and the values in brackets represent the reversible capacities [183].

### 3. CONCLUSION

Several alternative materials have been developed in recent years to replace  $\text{LiCoO}_2$  as cathode materials for LIBs owing to its structural instability and performance degradation or failure. These novel cathode materials designed for future

high-performance LIBs are reviewed in this study under three broad categories: lithiated transition metal oxides, vanadium pentoxides, and polyanion-type materials. It has been demonstrated that controlled niobium doping can improve the structural stability and electrochemical performance of advanced  $\text{LiNi}_{0.5}\text{Co}_{0.2}\text{Mn}_{0.3}\text{O}_2$  cathode materials for the development of high energy density LIBs. High-capacity retention of 93.77% after 100 cycles at 1.0 C and enhanced rate performance with  $125.5 \text{ mAh g}^{-1}$  at 5.0 C was delivered by Nb-doped  $\text{LiNi}_{0.5}\text{Co}_{0.2}\text{Mn}_{0.3}\text{O}_2$  materials. Coating LNCMO with LVMP can reduce the residual Li compounds on the surface and prevent the dissolution of transition metals during cycling. The as-synthesised LNCMO@LVMP compounds delivered a discharge capacity of  $300 \text{ mAh g}^{-1}$  with a high initial coulombic efficiency (84.2%) and excellent cycling stability. Moreover, the adverse effects of increased Ni content of NCA were mitigated by using the proposed co-precipitation technique with the merits of high tap density, stable reactivity of microspheres, and high activity with short paths for ion/electron diffusion of nanoparticles. The as-prepared  $\text{LiNi}_{0.9}\text{Co}_{0.07}\text{Al}_{0.03}\text{O}_2$  demonstrated a remarkable high initial reversible capacity of  $236 \text{ mAh g}^{-1}$  at 0.1 C and good cycling performance (with capacity retention of 93.1% after 100 cycles at 1 C and 86.3% after 200 cycles at 2 C). Additionally, the sample displayed superior cyclic stability at elevated temperatures of 45, 55, and 60 °C.

The structural stability of Ni-rich materials can be enhanced by decreasing cationic mixing and inhibiting interfacial side reactions, such as lattice doping and surface reconstruction. The rare earth element Ce derived from cerous nitrate – an economically and environmentally friendly raw material – has proven effective in reinforcing the interface of Ni-rich  $\text{LiNi}_{0.8}\text{Co}_{0.1}\text{Mn}_{0.1}\text{O}_2$  cathode materials for LIBs under high operating voltage. For instance, the 50<sup>th</sup> capacity of  $\text{LiNi}_{0.8}\text{Co}_{0.1}\text{Mn}_{0.1}\text{O}_2$  at 0.2 C within 2.75–4.5 V was improved from  $178.7 \text{ mAh g}^{-1}$  (89.8%) to  $196.8 \text{ mAh g}^{-1}$  (99.2%) after Ce salt modification at 600 °C. Additionally, the GN-LPO-NCM811 modified sample, with enhanced thermal stability, high ionic conductivity, and excellent electronic conductivity, offers a template for engineering the surface of Ni-rich NCM cathode materials of the future. A structure gradient  $\text{LiNi}_{0.8}\text{Co}_{0.1}\text{Mn}_{0.1}\text{O}_2$  cathode material synthesised by a secondary co-precipitation method exhibited a high compaction density and superior rate performance.

Porous hollow  $\text{V}_2\text{O}_5$  nanotubes (VNTs) as cathode materials for LIBs can improve the penetration of electrolyte, increase the contact surface area between electrolyte and active material and accommodate the volume variations via additional void space during cycling. The  $\text{V}_2\text{O}_5/n\text{H}_2\text{O}/\text{rGO}$  cathode material for LIBs displayed a high reversible capacity of  $268 \text{ mAh g}^{-1}$  at  $100 \text{ mA g}^{-1}$  and an excellent rate capability ( $196 \text{ mAh g}^{-1}$  at  $1000 \text{ mA g}^{-1}$  and  $129 \text{ mAh g}^{-1}$  at  $2000 \text{ mA g}^{-1}$ ), surpassing those of the  $\text{V}_2\text{O}_5/\text{carbon}$  composites reported in the literatures. The as-synthesised  $\text{V}_2\text{O}_5$  nanoflowers arrays on PRC demonstrated high-rate capability and excellent cycling stability, thereby qualifying them as high-performance cathode materials for LIBs.

Boracic polyanion doping significantly improved the rate capabilities and cycling stability of the NCM cathode materials due to the crystal structure's stabilization. The modified NCM cathode materials exhibited superior rate property at high current density ( $131.02 \text{ mAh g}^{-1}$  at 5 C) compared to the bare NCM ( $115.96 \text{ mAh g}^{-1}$  at 5 C) and higher

capacity retention (76.07% after 100 cycles at 1 C) than the bare NCM (59.15% after 100 cycles at 1 C). Moreover,  $B_2O_3$ - $LiNi_{0.94}Co_{0.06}O_2$  (B-NC) cathode materials for high-energy-density LIBs delivered a discharge capacity of  $223 \text{ mA h g}^{-1}$  at C/3 with 80% capacity retention after 400 cycles, superior to 61% retention for the bare  $LiNi_{0.94}Co_{0.06}O_2$ . The improved cyclability is credited to the development of a well-passivated boron/phosphorus-rich cathode-electrolyte interphase in B-NC. Remarkable progress has been made in improving the crystal structure stability and electrochemical performances of transition metal-based cathode materials for high-performance LIBs. However, further enhancements of the cathode materials are still feasible through engineering the electrode composition, microstructure, and morphology.

## REFERENCES

- [1] R. Chen, T. Zhao, X. Zhang, L. Liab and F. Wu, "Advanced cathode materials for lithium-ion batteries using," *Nanoscale Horizons*, vol. 1, no. 6, pp. 423-444, 2016.
- [2] H. Yu and H. Zhou, "High-Energy Cathode Materials ( $Li_2MnO_3$ - $LiMO_2$ ) for Lithium-Ion Batteries," *J. Phys. Chem. Lett.*, vol. 4, pp. 1268-1280, 2013.
- [3] C. Liu, F. Li, L. Ma and H. Cheng, "Advanced materials for energy storage," *Advanced materials*, vol. 22, no. 8, pp. E28-E62, 2010.
- [4] Y. Sun, S. Myung, B. Park, J. Prakash, I. Belharouak and K. Amine, "High-energy cathode material for long-life and safe lithium batteries," *Nature materials*, vol. 8, no. 4, pp. 320-324, 2009.
- [5] J. Yao, Y. Li, R. Massé, E. Uchaker and G. Cao, "Revitalized interest in vanadium pentoxide as cathode material for lithium-ion batteries and beyond," *Energy Storage Materials*, vol. 11, pp. 205-259, 2018.
- [6] F. Cheng, J. Liang, Z. Tao and J. Chen, "Functional Materials for Rechargeable Batteries," *Adv. Mater.*, vol. 23, pp. 1695-1715, 2011.
- [7] J. Tarascon and M. Armand, "Issues and challenges facing rechargeable lithium batteries," *Nature*, vol. 414, pp. 359-367, 2001.
- [8] A. Soge, "Anode Materials for Lithium-based Batteries: A review," *Journal of Materials Science Research and Reviews*, vol. 5, no. 3, pp. 21-39, 2020.
- [9] X. Rui, Q. Yan, M. Skyllas-Kazacos and T. Lim, " $Li_3V_2(PO_4)_3$  cathode materials for lithium-ion batteries: a review," *Journal of Power Sources*, vol. 258, pp. 19-38, 2014.
- [10] K. Mizushima, P. Jones, P. Wiseman and J. Goodenough, " $Li_xCoO_2$  ( $0 < x < 1$ ): A new cathode material for batteries of high energy density. 15(6)," *Materials Research Bulletin*, vol. 15, no. 6, pp. 783-789, 1980.
- [11] J. Reimers and J. Dahn, "Electrochemical and in situ X-ray diffraction studies of lithium intercalation in  $Li_xCoO_2$ ," *Journal of the Electrochemical Society*, 139(8), 2091., vol. 139, no. 8, p. 2091, 1992.
- [12] O. Compton, A. Abouimrane, Z. An, M. Palmeri, L. Brinson, K. Amine and S. Nguyen, "Exfoliation and reassembly of cobalt oxide nanosheets into a reversible lithium-ion battery cathode," *Small*, vol. 8, no. 7, pp. 1110-1116, 2012.
- [13] X. Pu and C. Yu, "Enhanced overcharge performance of nano- $LiCoO_2$  by novel  $Li_3VO_4$  surface coatings," *Nanoscale*, vol. 4, no. 21, pp. 6743-6747, 2012.
- [14] E. Antolini, "LiCoO<sub>2</sub>: formation, structure, lithium and oxygen nonstoichiometry, electrochemical behaviour and transport properties," *Solid state ionics*, vol. 170, no. 3-4, pp. 159-171, 2004.
- [15] J. Fergus, "Recent developments in cathode materials for lithium ion batteries," *Journal of Power Sources*, vol. 195, pp. 939-954, 2010.
- [16] D. Belov and M. Yang, "Investigation of the kinetic mechanism in overcharge process for Li-ion battery," *Solid State Ionics*, vol. 179, no. 27-32, pp. 1816-1821, 2008.
- [17] D. Belov and M. Yang, "Failure mechanism of Li-ion battery at overcharge conditions," *J. Solid State Electrochem.*, vol. 12, pp. 885-894, 2008.
- [18] C. Doh, D. Kim, H. Kim, H. Shin, Y. Jeong, S. Moon, B. Jin, S. Eom and et al., "Thermal and electrochemical behaviour of C/LixCoO<sub>2</sub> cell during safety test," *Journal of Power Sources*, vol. 175, pp. 881-885, 2008.
- [19] T. Ohzuku and Y. Makimura, "Layered lithium insertion material of  $LiCo_{1/3}Ni_{1/3}Mn_{1/3}O_2$  for lithium-ion batteries," *Chemistry Letters*, vol. 30, no. 7, pp. 642-643, 2001.
- [20] C. Yang, J. Huang, L. Huang and G. Wang, "Electrochemical performance of  $LiCo_{1/3}Mn_{1/3}Ni_{1/3}O_2$  hollow spheres as cathode material for lithium ion batteries," *Journal of power sources*, vol. 226, pp. 219-222, 2013.
- [21] J. Choi and A. Manthiram, "Investigation of the Irreversible Capacity Loss in the Layered  $LiNi_{1/3}Mn_{1/3}Co_{1/3}O_2$  Cathodes," *Electrochemical and Solid State Letters*, vol. 8, no. 8, p. C102, 2005.
- [22] J. Tarascon, E. Wang, F. Shokoohi, W. McKinnon and S. Colson, "The spinel phase of  $LiMn_2O_4$  as a cathode in secondary lithium cells," *Journal of the Electrochemical Society*, vol. 138, no. 10, p. 2859, 1991.
- [23] Y. Wu, Z. Wen, H. Feng and J. Li, "Hollow porous  $LiMn_2O_4$  microcubes as rechargeable lithium battery cathode with high electrochemical performance," *Small*, vol. 8, no. 6, pp. 858-862, 2012.
- [24] W. Tang, Y. Hou, F. Wang, L. Liu, Y. Wu and K. Zhu, " $LiMn_2O_4$  nanotube as cathode material of second-level charge capability for aqueous rechargeable batteries," *Nano letters*, vol. 13, no. 5, pp. 2036-2040, 2013.
- [25] R. Gummow, A. De Kock and M. Thackeray, "Improved capacity retention in rechargeable 4 V lithium/lithium-manganese oxide (spinel) cells," *Solid State Ionics*, vol. 69, no. 1, pp. 59-67, 1994.
- [26] B. Deng, H. Nakamura and M. Yoshio, "Capacity fading with oxygen loss for manganese spinels upon cycling at elevated temperatures," *Journal of power sources*, vol. 180, no. 2, pp. 864-868., 2008.

- [27] K. Chung and K. Kim, "Investigations into capacity fading as a result of a Jahn–Teller distortion in 4 V LiMn<sub>2</sub>O<sub>4</sub> thin film electrodes.," *Electrochimica Acta*, vol. 49, no. 20, pp. 3327-3337., 2004.
- [28] A. Cao, J. Hu, H. Liang and L. Wan, "Self-assembled vanadium pentoxide (V<sub>2</sub>O<sub>5</sub>) hollow microspheres from nanorods and their application in lithium-ion batteries," *Angewandte Chemie International Edition*, 44(28), , vol. 44, no. 28, pp. 4391-4395, 2005.
- [29] X. Rui, Z. Lu, H. Yu, D. Yang, H. Hng, T. Lim and Q. Yan, "Ultrathin V<sub>2</sub>O<sub>5</sub> nanosheet cathodes: realizing ultrafast reversible lithium storage," *Nanoscale*, vol. 5, no. 2, pp. 556-560, 2013.
- [30] Y. Wang and G. Cao, "Synthesis and enhanced intercalation properties of nanostructured vanadium oxides," *Chemistry of Materials*, vol. 18, no. 12, pp. 2787-2804., 2006.
- [31] G. Wang, X. Lu, Y. Ling, T. Zhai, H. Wang, Y. Tong and Y. Li, "LiCl/PVA gel electrolyte stabilizes vanadium oxide nanowire electrodes for pseudocapacitors," *ACS nano*, vol. 6, no. 11, pp. 10296-10302, 2012.
- [32] X. Rui, J. Zhu, D. Sim, C. Xu, Y. Zeng, H. Hng and Q. Yan, "Reduced graphene oxide supported highly porous V<sub>2</sub>O<sub>5</sub> spheres as a high-power cathode material for lithium ion batteries," *Nanoscale*, vol. 3, no. 11, pp. 4752-4758, 2011.
- [33] A. Padhi, K. Nanjundaswamy and J. Goodenough, "Phospho-olivines as positive-electrode materials for rechargeable lithium batteries," *Journal of the electrochemical society*, vol. 144, no. 4, p. 1188, 1997.
- [34] A. Yamada, N. Iwane, Y. Harada, S. Nishimura, Y. Koyama and I. Tanaka, "Lithium Iron Borates as High-Capacity Battery Electrodes," *Advanced Materials*, vol. 22, no. 32, pp. 3583-3587, 2010.
- [35] N. Recham, J. Chotard, L. Dupont, C. Delacourt, W. Walker, M. Armand and J. Tarascon, "A 3.6 V lithium-based fluorosulphate insertion positive electrode for lithium-ion batteries," *Nature materials*, vol. 9, no. 1, pp. 68-74, 2010.
- [36] M. Ati, M. Sougrati, G. Rouse, N. Recham, M. Doublet, J. Jumas and J. Tarascon, "Single-Step Synthesis of FeSO<sub>4</sub>F<sub>1-y</sub>OH<sub>y</sub> (0 ≤ y ≤ 1) Positive Electrodes for Li-Based Batteries," *Chemistry of Materials*, vol. 24, no. 8, pp. 1472-1485, 2012.
- [37] P. Barpanda, M. Ati, B. Melot, G. Rouse, J. Chotard, M. Doublet, M. Sougrati, S. Corr and et al., "A 3.90 V iron-based fluorosulphate material for lithium-ion batteries crystallizing in the triplite structure," *Nature Materials*, vol. 10, pp. 772-779, 2011.
- [38] A. Nytén, A. Abouimrane, M. Armand, T. Gustafsson and J. Thomas, "Electrochemical performance of Li<sub>2</sub>FeSiO<sub>4</sub> as a new Li-battery cathode material," *Electrochemistry communications*, vol. 7, no. 2, pp. 156-160, 2005.
- [39] M. Islam, R. Dominko, C. Masquelier, C. Sirisopanaporn, A. Armstrong and P. Bruce, "Silicate cathodes for lithium batteries: alternatives to phosphates?," *Journal of Materials Chemistry*, vol. 21, no. 27, pp. 9811-9818, 2011.
- [40] D. Rangappa, K. Murukanahally, T. Tomai, A. Unemoto and I. Honma, "Ultrathin nanosheets of Li<sub>2</sub>MSiO<sub>4</sub> (M= Fe, Mn) as high-capacity Li-ion battery electrode," *Nano letters*, vol. 12, no. 3, pp. 1146-1151, 2012.
- [41] D. Lv, J. Bai, P. Zhang, S. Wu, Y. Li, W. Wen, Z. Jiang, J. Mi and et al., "Understanding the high capacity of Li<sub>2</sub>FeSiO<sub>4</sub>: in situ XRD/XANES study combined with first-principles calculations," *Chemistry of Materials*, 25(10), 2014-2020., vol. 25, no. 10, pp. 2014-2020, 2013.
- [42] D. Cogswell and M. Bazant, "Coherency strain and the kinetics of phase separation in LiFePO<sub>4</sub> nanoparticles," *ACS nano*, vol. 6, no. 3, pp. 2215-2225, 2012.
- [43] S. Chung, J. Bloking and Y. Chiang, "Electronically conductive phospho-olivines as lithium storage electrodes," *Nature materials*, vol. 1, no. 2, pp. 123-128, 2002.
- [44] B. Kang and G. Ceder, "Battery materials for ultrafast charging and discharging," *Nature*, vol. 458, no. 7235, pp. 190-193, 2009.
- [45] J. Wang and X. Sun, "Understanding and recent development of carbon coating on LiFePO<sub>4</sub> cathode materials for lithium-ion batteries," *Energy & Environmental Science*, vol. 5, no. 1, pp. 5163-5185, 2012.
- [46] W. Zhang, "Structure and performance of LiFePO<sub>4</sub> cathode materials: A review," *Journal of Power Sources*, vol. 196, no. 6, pp. 2962-2970, 2011.
- [47] K. Zaghib, A. Guerfi, P. Hovington, A. Vijh, M. Trudeau, A. Mauger, J. Goodenough and C. Julien, "Review and analysis of nanostructured olivine-based lithium rechargeable batteries: Status and trends," *Journal of Power Sources*, vol. 232, p. 35, 2013.
- [48] D. Carriazo, M. Rossell, G. Zeng, I. Bilecka, R. Erni and M. Niederberger, "Formation Mechanism of LiFePO<sub>4</sub> Sticks Grown by a Microwave-Assisted Liquid-Phase Process.," *Small*, vol. 8, no. 14, pp. 2231-2238, 2012.
- [49] Y. Wang, Y. Wang, E. Hosono, K. Wang and H. Zhou, "The design of a LiFePO<sub>4</sub>/carbon nanocomposite with a core–shell structure and its synthesis by an in situ polymerization restriction method," *Angewandte Chemie International Edition*, vol. 47, no. 39, pp. 7461-7465, 2008.
- [50] M. Pivko, M. Bele, E. Tchernychova, N. Logar, R. Dominko and M. Gaberscek, "Synthesis of nanometric LiMnPO<sub>4</sub> via a two-step technique," *Chemistry of Materials*, vol. 24, no. 6, pp. 1041-1047, 2012.
- [51] N. Bramnik, K. Nikolowski, C. Baecht, K. Bramnik and H. Ehrenberg, "Phase transitions occurring upon lithium insertion– extraction of LiCoPO<sub>4</sub>," *Chemistry of Materials*, vol. 19, no. 4, pp. 908-915, 2007.
- [52] J. Wolfenstine and J. Allen, "Ni<sup>3+</sup>/Ni<sup>2+</sup> redox potential in LiNiPO<sub>4</sub>," *Journal of Power Sources*, vol. 14, no. 1-2, pp. 389-390, 2005.

- [53] M. Saïdi, J. Barker, H. Huang, J. Swoyer and G. Adamson, "Electrochemical properties of lithium vanadium phosphate as a cathode material for lithium-ion batteries," *Electrochemical and Solid State Letters*, vol. 5, no. 7, p. A149, 2002.
- [54] S. Megahed and B. Scrosati, "Lithium-ion rechargeable batteries," *Journal of Power Sources*, vol. 51, no. 1-2, pp. 79-104, 1994.
- [55] D. Guyomard and J. Tarascon, "Rocking-chair or lithium-ion rechargeable lithium batteries," *Advanced materials*, vol. 6, no. 5, pp. 408-412, 1994.
- [56] K. Xu, "Nonaqueous liquid electrolytes for lithium-based rechargeable batteries. 104(10), 4303-4418.," *Chemical reviews*, vol. 104, no. 10, pp. 4303-4418, 2004.
- [57] Y. Wang and G. Cao, "Developments in nanostructured cathode materials for high-performance lithium-ion batteries," *Advanced materials*, vol. 20, no. 12, pp. 2251-2269., 2008.
- [58] Y. Guo, J. Hu and L. Wan, "Nanostructured materials for electrochemical energy conversion and storage devices," *Advanced Materials*, vol. 20, no. 15, pp. 2878-2887, 2008.
- [59] S. Megahed and W. Ebner, "Lithium-ion battery for electronic applications," *Journal of Power Sources*, vol. 54, no. 1, pp. 155-162, 1995.
- [60] F. Cheng, J. T. Z. Liang and J. Chen, "Functional materials for rechargeable batteries," *Advanced Materials*, vol. 23, no. 15, pp. 1695-1715, 2011.
- [61] D. Guyomard, "Advanced cathode materials for lithium batteries batteries, in: Energy Storage Systems for Electronics," in *New Trends in Electrochemical Technology*, vol. 1, T. Osaka and M. Datta, Eds., Amsterdam, Gordon and Breach, 2000, pp. 253-350.
- [62] M. Whittingham, "Lithium batteries and cathode materials," *Chemical reviews*, vol. 104, no. 10, pp. 4271-4302, 2004.
- [63] D. Wang, X. Li, Z. Wang, H. Guo, Y. Xu, Y. Fan and J. Ru, "Role of zirconium dopant on the structure and high voltage electrochemical performances of LiNi<sub>0.5</sub>Co<sub>0.2</sub>Mn<sub>0.3</sub>O<sub>2</sub> cathode materials for lithium ion batteries," *Electrochimica Acta*, vol. 188, pp. 48-56, 2016.
- [64] Y. Huang, F. Jin, F. Chen and L. Chen, "Improved cycle stability and high-rate capability of Li<sub>3</sub>VO<sub>4</sub>-coated Li [Ni<sub>0.5</sub>Co<sub>0.2</sub>Mn<sub>0.3</sub>] O<sub>2</sub> cathode material under different voltages," *Journal of Power Sources*, vol. 256, pp. 1-7, 2014.
- [65] X. Xiong, D. Ding, Y. Bu, Z. Wang, B. Huang, H. Guo and X. Li, "Enhanced electrochemical properties of a LiNiO<sub>2</sub>-based cathode material by removing lithium residues with (NH<sub>4</sub>)<sub>2</sub>HPO<sub>4</sub>," *Journal of Materials Chemistry A*, vol. 2, p. 11691, 2014.
- [66] Z. Wang, S. Huang, B. Chen, H. Wu and Y. Zhang, "Infiltrative coating of LiNi<sub>0.5</sub>Co<sub>0.2</sub>Mn<sub>0.3</sub>O<sub>2</sub> microspheres with layer-structured LiTiO<sub>2</sub>: towards superior cycling performances for Li-ion batteries," *Journal of Materials Chemistry A*, vol. 2, no. 47, pp. 19983-19987, 2014.
- [67] F. Wu, J. Tian, Y. Su, Y. Guan, Y. Jin, Z. Wang, T. He and L. Bao, "Lithium-active molybdenum trioxide coated LiNi<sub>0.5</sub>Co<sub>0.2</sub>Mn<sub>0.3</sub>O<sub>2</sub> cathode material with enhanced electrochemical properties for lithium-ion batteries," *Journal of Power Sources*, vol. 269, pp. 747-754, 2014.
- [68] D. Wang, X. Li, Z. Wang, H. Guo, Z. Huang, L. Kong and J. Ru, "Improved high voltage electrochemical performance of Li<sub>2</sub>ZrO<sub>3</sub>-coated LiNi<sub>0.5</sub>Co<sub>0.2</sub>Mn<sub>0.3</sub>O<sub>2</sub> cathode material," *Journal of Alloys and Compounds*, vol. 647, pp. 612-619, 2015.
- [69] D. Wang, X. Li, Z. Wang, H. Guo, X. Chen, X. Zheng, Y. Xu and J. Ru, "Multifunctional Li<sub>2</sub>O-2B<sub>2</sub>O<sub>3</sub> coating for enhancing high voltage electrochemical performances and thermal stability of layered structured LiNi<sub>0.5</sub>Co<sub>0.2</sub>Mn<sub>0.3</sub>O<sub>2</sub> cathode materials for lithium ion batteries," *Electrochimica Acta*, vol. 174, pp. 1225-1233, 2015.
- [70] L. Li, Z. Chen, Q. Zhang, M. Xu, X. Zhou, H. Zhu and K. Zhang, "A hydrolysis-hydrothermal route for the synthesis of ultrathin LiAlO<sub>2</sub>-inlaid LiNi<sub>0.5</sub>Co<sub>0.2</sub>Mn<sub>0.3</sub>O<sub>2</sub> as a high-performance cathode material for lithium ion batteries," *Journal of Materials Chemistry A*, vol. 3, pp. 894-904, 2014.
- [71] X. Xiong, Z. Wang, G. Yan, H. Guo and X. Li, "Role of V<sub>2</sub>O<sub>5</sub> coating on LiNiO<sub>2</sub>-based materials for lithium ion battery," *Journal of Power Sources*, vol. 245, pp. 183-193, 2014.
- [72] K. Liu, G. Yang, Y. Dong, T. Shi and L. Chen, "Enhanced cycling stability and rate performance of Li [Ni<sub>0.5</sub>Co<sub>0.2</sub>Mn<sub>0.3</sub>] O<sub>2</sub> by CeO<sub>2</sub> coating at high cut-off voltage," *Journal of Power Sources*, vol. 281, pp. 370-377, 2015.
- [73] Z. Yang, W. Xiang, Z. Wu, F. He, J. Zhang, Y. Xiao, B. Zhong and X. Guo, "Effect of niobium doping on the structure and electrochemical performance of LiNi<sub>0.5</sub>Co<sub>0.2</sub>Mn<sub>0.3</sub>O<sub>2</sub> cathode materials for lithium ion batteries," *Ceramics International*, vol. 43, no. 4, pp. 3866-3872, 2017.
- [74] M. C. S. L. P. S. I. I. A. M. L. Fehse, D. Jones, J. Roziere, F. Fischer, C. Tessier and L. Stievano, "Nb-doped TiO<sub>2</sub> nanofibers for lithium ion batteries," *The Journal of Physical Chemistry C*, vol. 117, no. 27, pp. 13827-13835, 2013.
- [75] Y. Xia, W. Zhang, H. Huang, Y. Gan, C. Li and X. Tao, "Synthesis and electrochemical properties of Nb-doped Li<sub>3</sub>V<sub>2</sub>(PO<sub>4</sub>)<sub>3</sub>/C cathode materials for lithium-ion batteries," *Materials Science and Engineering: B*, vol. 176, no. 8, pp. 633-639, 2011.
- [76] B. Tian, H. Xiang, L. Zhang, Z. Li and H. Wang, "Niobium doped lithium titanate as a high rate anode material for Li-ion batteries," *Electrochimica Acta*, vol. 55, no. 19, pp. 5453-5458, 2010.
- [77] T. Yi, L. Yin, Y. Ma, H. Shen, Y. Zhu and R. Zhu, "Lithium-ion insertion kinetics of Nb-doped LiMn<sub>2</sub>O<sub>4</sub> positive-electrode material," *Ceramics International*, vol. 39, no. 4, pp. 4673-4678, 2013.
- [78] J. Wu, H. Liu, X. Ye, J. Xia, Y. Lu, C. Lin and X. Yu, "Effect of Nb doping on electrochemical properties of LiNi<sub>1/3</sub>Co<sub>1/3</sub>Mn<sub>1/3</sub>O<sub>2</sub> at high cutoff voltage for

- lithium-ion battery," *Journal of Alloys and Compounds*, vol. 644, pp. 223-227, 2015.
- [79] L. Zhou, J. Liu, L. Huang, N. Jiang, Q. Zheng and D. Lin, "Sn-doped Li<sub>1.2</sub>Mn<sub>0.54</sub>Ni<sub>0.13</sub>Co<sub>0.13</sub>O<sub>2</sub> cathode materials for lithium-ion batteries with enhanced electrochemical performance," *Journal of Solid State Electrochemistry*, vol. 21, no. 12, pp. 3467-3477, 2017.
- [80] Y. Zhao, M. Xia, X. Hu, Z. Zhao, Y. Wang and Z. Lv, "Effects of Sn doping on the structural and electrochemical properties of Li<sub>1.2</sub>Ni<sub>0.2</sub>Mn<sub>0.8</sub>O<sub>2</sub> Li-rich cathode materials," *Electrochimica Acta*, vol. 174, p. 1167-1174, 2015.
- [81] Q. Qiao, L. Qin, G. Li, Y. Wang and X. Gao, "Sn-stabilized Li-rich layered Li (Li<sub>0.17</sub>Ni<sub>0.25</sub>Mn<sub>0.58</sub>)O<sub>2</sub> oxide as a cathode for advanced lithium-ion batteries," *Journal of Materials Chemistry A*, vol. 3, no. 34, pp. 17627-17634, 2015.
- [82] H. Zhang, F. Li, G. Pan, G. Li and X. Gao, "The effect of polyanion-doping on the structure and electrochemical performance of Li-rich layered oxides as cathode for lithium-ion batteries," *Journal of the Electrochemical Society*, vol. 162, no. 9, p. A1899, 2015.
- [83] S. Yang, P. Wang, H. Wei, L. Tang, X. Zhang, Z. He, Y. Li, H. Tong and et al., "Li<sub>4</sub>V<sub>2</sub>Mn(PO<sub>4</sub>)<sub>4</sub>-stabilized Li [Li<sub>0.2</sub>Mn<sub>0.54</sub>Ni<sub>0.13</sub>Co<sub>0.13</sub>]O<sub>2</sub> cathode materials for lithium ion batteries," *Nano Energy*, vol. 63, p. 103889, 2019.
- [84] S. Li, Z. Su and X. Wang, "High performance (1-x) LiMnPO<sub>4</sub>·xLi<sub>3</sub>V<sub>2</sub>(PO<sub>4</sub>)<sub>3</sub>/C composite cathode materials prepared by a sol-gel method," *RSC Advances*, 5(98), , vol. 5, no. 98, pp. 80170-80175, 2015.
- [85] J. Son, G. Kim, M. Kim, S. Kim, V. Aravindan, Y. Lee and Y. Lee, "Carbon coated NASICON type Li<sub>3</sub>V<sub>2</sub>-xM<sub>x</sub>(PO<sub>4</sub>)<sub>3</sub> (M= Mn, Fe and Al) materials with enhanced cyclability for Li-ion batteries," *Journal of The Electrochemical Society*, vol. 160, no. 1, p. A87, 2012.
- [86] P. Zhou, H. Meng, Z. Zhang, C. Chen, Y. Lu, J. Cao, F. Cheng and J. Chen, "Stable layered Ni-rich LiNi<sub>0.9</sub>Co<sub>0.07</sub>Al<sub>0.03</sub>O<sub>2</sub> microspheres assembled with nanoparticles as high-performance cathode materials for lithium-ion batteries," *Journal of Materials Chemistry A*, vol. 5, no. 6, pp. 2724-2731, 2017.
- [87] M. Jo, M. Noh, P. Oh, Y. Kim and J. Cho, "A New High Power LiNi<sub>0.81</sub>Co<sub>0.1</sub>Al<sub>0.09</sub>O<sub>2</sub> Cathode Material for Lithium-Ion Batteries," *Advanced Energy Materials*, vol. 4, no. 13, p. 1301583, 2014.
- [88] N. Wu, H. Wu, W. Yuan, S. Liu, J. Liao and Y. Zhang, "Facile synthesis of one-dimensional LiNi<sub>0.8</sub>Co<sub>0.15</sub>Al<sub>0.05</sub>O<sub>2</sub> microrods as advanced cathode materials for lithium ion batteries," *Journal of Materials Chemistry A*, vol. 3, no. 26, pp. 13648-13652, 2015.
- [89] A. Bhaskar, S. Krueger, V. Siozios, J. Li, S. Nowak and M. Winter, "Synthesis and Characterization of High-Energy, High-Power Spinel-Layered Composite Cathode Materials for Lithium-Ion Batteries," *Advanced Energy Materials*, vol. 5, no. 5, p. 1401156, 2015.
- [90] H. Xie, K. Du, G. Hu, J. Duan, Z. Peng, Z. Zhang and Y. Cao, "Synthesis of LiNi<sub>0.8</sub>Co<sub>0.15</sub>Al<sub>0.05</sub>O<sub>2</sub> with 5-sulfosalicylic acid as a chelating agent and its electrochemical properties," *Journal of Materials Chemistry A*, vol. 3, no. 40, pp. 20236-20243, 2015.
- [91] I. Belharouak, W. Lu, D. Vissers and K. Amine, "Safety characteristics of Li(Ni<sub>0.8</sub>Co<sub>0.15</sub>Al<sub>0.05</sub>)O<sub>2</sub> and Li(Ni<sub>1/3</sub>Co<sub>1/3</sub>Mn<sub>1/3</sub>)O<sub>2</sub>," *Electrochemistry Communications*, 8(2), , vol. 8, no. 2, pp. 329-335, 2006.
- [92] Z. Cabán-Huertas, O. Ayyad, D. Dubal and P. Gómez-Romero, "Aqueous synthesis of LiFePO<sub>4</sub> with fractal granularity.," *Scientific reports*, vol. 6, no. 1, pp. 1-9, 2016.
- [93] R. Amin, D. Ravnsbæk and Y. Chiang, "Characterization of electronic and ionic transport in Li<sub>1-x</sub>Ni<sub>0.8</sub>Co<sub>0.15</sub>Al<sub>0.05</sub>O<sub>2</sub> (NCA)," *Journal of The Electrochemical Society*, vol. 162, no. 7, p. A1163., 2015.
- [94] H. Noh, S. Youn, C. Yoon and Y. Sun, "Comparison of the structural and electrochemical properties of layered Li [Ni<sub>x</sub>Co<sub>y</sub>Mn<sub>z</sub>]O<sub>2</sub> (x= 1/3, 0.5, 0.6, 0.7, 0.8 and 0.85) cathode material for lithium-ion batteries," *Journal of power sources*, vol. 233, pp. 121-130, 2013.
- [95] D. Wan, Z. Fan, Y. Dong, E. Baasanjav, H. Jun, B. Jin, E. Jin and S. Jeong, "Effect of metal (Mn, Ti) doping on NCA cathode materials for lithium ion batteries," *Journal of Nanomaterials*, 2018.
- [96] Z. Deng and A. Manthiram, "Influence of cationic substitutions on the oxygen loss and reversible capacity of lithium-rich layered oxide cathodes," *The Journal of Physical Chemistry C*, vol. 115, no. 14, pp. 7097-7103, 2011.
- [97] H. Chen, J. Dawson and J. Harding, "Effects of cationic substitution on structural defects in layered cathode materials LiNiO<sub>2</sub>," *Journal of Materials Chemistry A*, vol. 2, no. 21, pp. 7988-7996., 2014.
- [98] F. Wu, Q. Li, L. Chen, Y. Lu, Y. Su, L. Bao, R. Chen and S. Chen, "Use of Ce to Reinforce the Interface of Ni-Rich LiNi<sub>0.8</sub>Co<sub>0.1</sub>Mn<sub>0.1</sub>O<sub>2</sub> Cathode Materials for Lithium-Ion Batteries under High Operating Voltage," *ChemSusChem*, vol. 12, no. 4, pp. 935-943, 2019.
- [99] S. Chen, T. He, Y. Su, Y. Lu, L. Bao, L. Chen, Q. Zhang, J. Wang and et al., "Ni-rich LiNi<sub>0.8</sub>Co<sub>0.1</sub>Mn<sub>0.1</sub>O<sub>2</sub> oxide coated by dual-conductive layers as high performance cathode material for lithium-ion batteries," *ACS applied materials & interfaces*, vol. 9, no. 35, pp. 29732-29743, 2017.
- [100] J. Kim, H. Lee, H. Cha, M. Yoon, M. Park and J. Cho, "Prospect and reality of Ni-Rich cathode for commercialization," *Advanced energy materials*, vol. 8, no. 6, p. 1702028, 2018.
- [101] D. Wang, R. Kou, Y. Ren, C. Sun, H. Zhao, M. Zhang, Y. Li, A. Huq and et al., "Synthetic control of kinetic reaction pathway and cationic ordering in high-Ni

- layered oxide cathodes," *Advanced Materials*, vol. 29, no. 39, p. 1606, 2017.
- [102] F. I. Lin, D. Nordlund, T. Weng, M. Asta, H. Xin and M. Doeff, "Surface reconstruction and chemical evolution of stoichiometric layered cathode materials for lithium-ion batteries," *Nature communications*, vol. 5, no. 1, pp. 1-9, 2014.
- [103] J. Reed and G. Ceder, "Role of electronic structure in the susceptibility of metastable transition-metal oxide structures to transformation," *Chemical reviews*, vol. 104, no. 10, pp. 4513-4534, 2004.
- [104] Y. Kim, D. Kim and S. Kang, "Experimental and first-principles thermodynamic study of the formation and effects of vacancies in layered lithium nickel cobalt oxides," *Chemistry of Materials*, vol. 23, no. 4, pp. 5388-5397, 2011.
- [105] P. Rozier and J. Tarascon, "Li-rich layered oxide cathodes for next-generation Li-ion batteries: chances and challenges," *Journal of The Electrochemical Society*, vol. 162, no. 14, p. A2490, 2015.
- [106] A. Manthiram, B. Song and W. Li, "A perspective on nickel-rich layered oxide cathodes for lithium-ion batteries," *Energy Storage Materials*, 6, 125-139, vol. 6, pp. 125-139, 2017.
- [107] W. Zhao, J. Zheng, L. Zou, H. Jia, B. Liu, H. Wang, M. Engelhard, C. Wang and et al., "High voltage operation of Ni-rich NMC cathodes enabled by stable electrode/electrolyte interphases," *Advanced energy materials*, vol. 8, no. 19, p. 1800297, 2018.
- [108] S. Woo, S. Myung, H. Bang, D. Kim and Y. Sun, "Improvement of electrochemical and thermal properties of Li [Ni<sub>0.8</sub>Co<sub>0.1</sub>Mn<sub>0.1</sub>] O<sub>2</sub> positive electrode materials by multiple metal (Al, Mg) substitution," *Electrochimica Acta*, vol. 54, no. 15, p. 385, 2009.
- [109] S. Woo, B. Park, C. Yoon, S. Myung, J. Prakash and Y. Sun, "Improvement of electrochemical performances of Li [Ni<sub>0.8</sub>Co<sub>0.1</sub>Mn<sub>0.1</sub>] O<sub>2</sub> cathode materials by fluorine substitution," *Journal of the Electrochemical Society*, vol. 154, no. 7, p. A64, 2007.
- [110] H. Kim, S. Myung, J. Lee and Y. Sun, "Effects of manganese and cobalt on the electrochemical and thermal properties of layered Li [Ni<sub>0.52</sub>Co<sub>0.16</sub>+xMn<sub>0.32-x</sub>] O<sub>2</sub> cathode materials," *Journal of Power Sources*, vol. 196, no. 16, pp. 6710-6715, 2011.
- [111] J. Zheng, W. Kan and A. Manthiram, "Role of Mn Content on the Electrochemical Properties of Nickel-Rich Layered LiNi<sub>0.8-x</sub>Co<sub>0.1</sub>Mn<sub>0.1+x</sub>O<sub>2</sub> (0.0 ≤ x ≤ 0.08) Cathodes for Lithium-Ion Batteries," *ACS applied materials & interfaces*, vol. 7, no. 12, pp. 6926-6934, 2015.
- [112] F. Wu, Q. Li, L. Bao, Y. Zheng, Y. Lu, Y. Su, J. Wang, S. Chen and et al., "Role of LaNiO<sub>3</sub> in suppressing voltage decay of layered lithium-rich cathode materials," *Electrochimica Acta*, vol. 260, pp. 986-993, 2018.
- [113] Y. Huang, F. Jin, F. Chen and L. Chen, "Improved cycle stability and high-rate capability of Li<sub>3</sub>VO<sub>4</sub>-coated Li [Ni<sub>0.5</sub>Co<sub>0.2</sub>Mn<sub>0.3</sub>] O<sub>2</sub> cathode material under different voltages," *Journal of Power Sources*, vol. 256, pp. 1-7, 2014.
- [114] H. Ha, N. Yun, M. Kim, M. Woo and K. Kim, "Enhanced electrochemical and thermal stability of surface-modified LiCoO<sub>2</sub> cathode by CeO<sub>2</sub> coating," *Electrochimica Acta*, vol. 51, no. 16, pp. 3297-3302, 2006.
- [115] H. Ha, N. Yun and K. Kim, "Improvement of electrochemical stability of LiMn<sub>2</sub>O<sub>4</sub> by CeO<sub>2</sub> coating for lithium-ion batteries," *Electrochimica Acta*, vol. 52, no. 9, pp. 3236-3241, 2007.
- [116] Y. Zhang, S. Xia, Y. Zhang, P. Dong, Y. Yan and R. Yang, "Ce-doped LiNi<sub>1/3</sub>Co<sub>(1/3-x/3)</sub>Mn<sub>1/3</sub>Ce<sub>x/3</sub>O<sub>2</sub> cathode materials for use in lithium ion batteries," *Chinese Science Bulletin*, vol. 57, no. 32, pp. 4181-4187, 2012.
- [117] Z. Wu and Y. Zhou, "Effect of Ce-doping on the structure and electrochemical performance of lithium trivanadate prepared by a citrate sol-gel method," *Journal of Power Sources*, vol. 199, pp. 300-307, 2012.
- [118] D. Arumugam and G. Kalaignan, "Synthesis and electrochemical characterizations of nano size Ce doped LiMn<sub>2</sub>O<sub>4</sub> cathode materials for rechargeable lithium batteries," *Journal of Electroanalytical Chemistry*, vol. 648, no. 1, pp. 54-59, 2010.
- [119] S. Zhong, W. You, L. Jiequn, W. Kang and L. Fan, "Synthesis and electrochemical properties of Ce-doped LiNi<sub>1/3</sub>Mn<sub>1/3</sub>Co<sub>1/3</sub>O<sub>2</sub> cathode material for Li-ion batteries," *Journal of Rare Earths*, vol. 29, no. 9, pp. 891-895, 2011.
- [120] Q. Fan, S. Yang, J. Liu, H. Liu, K. Lin, R. Liu, C. Hong, L. Liu and et al., "Mixed-conducting interlayer boosting the electrochemical performance of Ni-rich layered oxide cathode materials for lithium ion batteries," *Journal of Power Sources*, vol. 421, pp. 91-99, 2019.
- [121] Y. Ding, B. Deng, H. Wang, X. Li, T. Chen, X. Yan, Q. Wan, M. Qu and et al., "Improved electrochemical performances of LiNi<sub>0.6</sub>Co<sub>0.2</sub>Mn<sub>0.2</sub>O<sub>2</sub> cathode material by reducing lithium residues with the coating of Prussian blue," *Journal of Alloys and Compounds*, vol. 774, pp. 451-460, 2019.
- [122] C. Jo, D. Cho, H. Noh, H. Yashiro, Y. Sun and S. Myung, "An effective method to reduce residual lithium compounds on Ni-rich Li [Ni<sub>0.6</sub>Co<sub>0.2</sub>Mn<sub>0.2</sub>] O<sub>2</sub> active material using a phosphoric acid derived Li<sub>3</sub>PO<sub>4</sub> nanolayer," *Nano Research*, vol. 8, no. 5, pp. 1464-1479, 2015.
- [123] X. Xiong, D. Ding, Y. Bu, Z. Wang, B. Huang, H. Guo and X. Li, "Enhanced electrochemical properties of a LiNiO<sub>2</sub>-based cathode material by removing lithium residues with (NH<sub>4</sub>)<sub>2</sub>HPO<sub>4</sub>," *Journal of Materials Chemistry A*, vol. 2, no. 30, pp. 11691-11696, 2014.
- [124] Y. Su, G. Chen, L. Chen, Y. Lu, Q. Zhang, Z. Lv, C. Li, L. Li and et al., "High-rate structure-gradient Ni-rich cathode material for lithium-ion batteries," *ACS applied materials & interfaces*, vol. 11, no. 40, pp. 36697-36704, 2019.

- [125] S. H. T. Chen, Y. Su, Y. Lu, L. Bao, L. Chen, Q. Zhang, J. Wang and et al., "Ni-rich  $\text{LiNi}_0.8\text{Co}_0.1\text{Mn}_0.1\text{O}_2$  oxide coated by dual-conductive layers as high performance cathode material for lithium-ion batteries," *ACS applied materials & interfaces*, vol. 9, no. 35, pp. 29732-29743, 2017.
- [126] Y. Zhang, X. Yuan, T. Lu, Z. Gong, L. Pan and S. Guo, "Hydrated vanadium pentoxide/reduced graphene oxide composite cathode material for high-rate lithium ion batteries," *Journal of Colloid and Interface Science*, vol. 585, pp. 347-354, 2021.
- [127] L. Wang, Y. Wang, X. Zhu and Y. Zhao, "Conventional synthesis of  $\text{V}_2\text{O}_5$ /graphite composites with enhanced lithium ion storage," *Journal of Alloys and Compounds*, vol. 792, pp. 418-423, 2019.
- [128] S. Wang, K. Owusu, L. Mai, Y. Ke, Y. Zhou, P. Hu, S. Magdassi and Y. Long, "Vanadium dioxide for energy conservation and energy storage applications: Synthesis and performance improvement," *Applied Energy*, vol. 211, pp. 200-217, 2018.
- [129] Y. Yue and H. Liang, "Micro-and nano-structured vanadium pentoxide ( $\text{V}_2\text{O}_5$ ) for electrodes of lithium-ion batteries," *Advanced Energy Materials*, vol. 7, no. 17, p. 1602545, 2017.
- [130] Y. Zhang, Y. Luo, C. Fincher, S. Banerjee and M. Pharr, "Chemo-mechanical degradation in  $\text{V}_2\text{O}_5$  thin film cathodes of Li-ion batteries during electrochemical cycling," *Journal of Materials Chemistry A*, vol. 7, no. 41, pp. 23922-23930, 2019.
- [131] C. Zhang, Z. Chen, Z. Guo and X. Lou, "Additive-free synthesis of 3D porous  $\text{V}_2\text{O}_5$  hierarchical microspheres with enhanced lithium storage properties," *Energy & Environmental Science*, vol. 6, no. 3, pp. 974-978, 2013.
- [132] X. Rui, Z. Lu, H. Yu, D. Yang, H. Hng, T. Lim and Q. Yan, "Ultrathin  $\text{V}_2\text{O}_5$  nanosheet cathodes: realizing ultrafast reversible lithium storage," *Nanoscale*, vol. 5, no. 2, pp. 556-560, 2013.
- [133] N. Wu, W. Du, G. Liu, Z. Zhou, H. Fu, Q. Tang, X. Liu and Y. He, "Synthesis of hierarchical sisal-like  $\text{V}_2\text{O}_5$  with exposed stable {001} facets as long life cathode materials for advanced lithium-ion batteries," *ACS applied materials & interfaces*, vol. 9, no. 50, pp. 43681-43687, 2017.
- [134] D. Kong, X. Li, Y. Zhang, X. Hai, B. Wang, X. Qiu, Q. Song, Q. Yang and et al., "Encapsulating  $\text{V}_2\text{O}_5$  into carbon nanotubes enables the synthesis of flexible high-performance lithium ion batteries," *Energy & Environmental Science*, vol. 9, no. 3, p. 90, 2016.
- [135] M. Ihsan, Q. Meng, L. Li, D. Li, H. Wang, K. Seng, Z. Chen, S. Kennedy and et al., " $\text{V}_2\text{O}_5$ /Mesoporous Carbon Composite as a Cathode Material for Lithium-Ion Batteries," *Electrochimica Acta*, vol. 173, pp. 172-177, 2015.
- [136] Y. Yang, L. Li, H. Fei, Z. Peng, G. Ruan and J. Tour, "Graphene nanoribbon/ $\text{V}_2\text{O}_5$  cathodes in lithium-ion batteries," *ACS applied materials & interfaces*, vol. 6, no. 12, pp. 9590-9594, 2014.
- [137] L. Mai, F. Dong, X. Xu, Y. Luo, Q. An, Y. Zhao, J. Pan and J. Yang, "Cucumber-Like  $\text{V}_2\text{O}_5$ /poly(3,4-Ethylenedioxythiophene)& $\text{MnO}_2$  Nanowires with Enhanced Electrochemical Cyclability," *Nano Letters*, vol. 13, pp. 740-745, 2013.
- [138] L. Mai, L. Xu, C. Han, X. Xu, Y. Luo, S. Zhao and Y. Zhao, "Electrospun Ultralong Hierarchical Vanadium Oxide Nanowires with High Performance for Lithium Ion Batteries," *Nano Letters*, vol. 10, pp. 4750-4755, 2010.
- [139] A. Ramasami, M. Reddy, P. Nithyadharseni, B. Chowdari and G. Balakrishna, "Gel-combustion synthesised vanadium pentoxide nanowire clusters for rechargeable lithium batteries," *Journal of Alloys and Compounds*, vol. 695, pp. 850-858, 2017.
- [140] X. Rui, Y. Tang, O. Malyi, A. Gusak, Y. Zhang, Z. Niu, H. Tan, C. Persson and et al., "Ambient dissolution-recrystallization towards large-scale preparation of  $\text{V}_2\text{O}_5$  nanobelts for high-energy battery applications. Nano," *Nano Energy*, vol. 22, pp. 583-593, 2016.
- [141] Y. Yang, L. Li, H. Fei, Z. Peng, G. Ruan and J. Tour, "Graphene nanoribbon/ $\text{V}_2\text{O}_5$  cathodes in lithium-ion batteries," *ACS applied materials & interfaces*, vol. 6, no. 12, pp. 9590-9594, 2014.
- [142] X. Peng, X. Zhang, L. Wang, L. Hu, S. Cheng, C. Huang, B. Gao, F. Ma and et al., "Hydrogenated  $\text{V}_2\text{O}_5$  nanosheets for superior lithium storage properties," *Advanced Functional Materials*, vol. 26, no. 5, pp. 784-791, 2016.
- [143] Y. Li, J. Yao, E. Uchaker, J. Yang, Y. Huang, M. Zhang and G. Cao, "Leaf-Like  $\text{V}_2\text{O}_5$  Nanosheets Fabricated by a Facile Green Approach as High Energy Cathode Material for Lithium-Ion Batteries," *Advanced Energy Materials*, vol. 3, no. 9, pp. 1171-1175, 2013.
- [144] X. Rui, Z. Lu, H. Yu, D. Yang, H. Hng, T. Lim and Q. Yan, "Ultrathin  $\text{V}_2\text{O}_5$  nanosheet cathodes: realizing ultrafast reversible lithium storage," *Nanoscale*, vol. 5, no. 2, pp. 556-560, 2013.
- [145] L. Mai, Q. An, Q. Wei, J. Fei, P. Zhang, X. Xu, Y. Zhao, M. Yan and et al., "Nanoflakes-Assembled Three-Dimensional Hollow-Porous  $\text{V}_2\text{O}_5$  as Lithium Storage Cathodes with High-Rate Capacity," *Small*, vol. 10, pp. 3032-3037, 2014.
- [146] H. Pang, P. Cheng, H. Yang, J. Lu, C. Guo, G. Ning and C. Li, "Template-Free Bottom-Up Synthesis of Yolk-Shell Vanadium Oxide as High Performance Cathode for Lithium Ion Batteries," *Chemical Communications*, vol. 49, no. 15, pp. 1536-1538, 2013.
- [147] A. Pan, H. Wu, L. Zhang and X. Lou, "Uniform  $\text{V}_2\text{O}_5$  nanosheet-assembled hollow microflowers with excellent lithium storage properties," *Energy & Environmental Science*, vol. 6, no. 5, pp. 1476-1479, 2013.
- [148] M. Sasidharan, N. Gunawardhana, M. Yoshio and K. Nakashima, " $\text{V}_2\text{O}_5$  hollow nanospheres: A lithium intercalation host with good rate capability and capacity retention," *Journal of the Electrochemical Society*, vol. 159, no. 5, p. A618, 2012.

- [149] P. Kumar and L. Hu, "Sulphur-reduced self-assembly of flower-like vanadium pentoxide as superior cathode material for Li-ion battery," *Journal of Alloys and Compounds*, 655, 79-85., vol. 655, pp. 79-85, 2016.
- [150] Y. Liu, D. Guan, G. Gao, X. Liang, W. Sun, K. Zhang, W. Bi and G. Wu, "Enhanced electrochemical performance of electrospun V<sub>2</sub>O<sub>5</sub> nanotubes as cathodes for lithium ion batteries," *Journal of Alloys and Compounds*, vol. 726, pp. 922-929, 2017.
- [151] H. Jiang, H. Chen, Y. Wei, J. Zeng, H. Liu, Y. Zhang and H. Wu, "Biotemplate-mediated structural engineering of rod-like V<sub>2</sub>O<sub>5</sub> cathode materials for lithium-ion batteries," *Journal of Alloys and Compounds*, vol. 787, pp. 625-630, 2019.
- [152] R. Raccichini, A. Varzi, S. Passerini and B. Scrosati, "(2015). The role of graphene for electrochemical energy storage," *Nature materials*, vol. 14, no. 3, pp. 271-279, 2015.
- [153] H. Chen, M. Müller, K. Gilmore, G. Wallace and D. Li, "Mechanically strong, electrically conductive, and biocompatible graphene paper," *Advanced Materials*, vol. 20, no. 18, pp. 3557-3561, 2008.
- [154] Y. Zhu, S. Murali, W. Cai, X. Li, J. Suk, J. Potts and R. Ruoff, "Graphene and graphene oxide: synthesis, properties, and applications," *Advanced materials*, vol. 22, no. 35, pp. 3906-3924, 2010.
- [155] S. Iijima and T. Ichihashi, "Single-shell carbon nanotubes of 1-nm diameter," *Nature*, vol. 363, no. 6430, pp. 603-605, 1993.
- [156] P. Ajayan and O. Zhou, "Applications of carbon nanotubes," *Carbon nanotubes*, pp. 391-425, 2001.
- [157] M. Endo, M. Strano and P. Ajayan, "Potential applications of carbon nanotubes," *Carbon nanotube*, pp. 13-62, 2007.
- [158] M. Krolow, C. Hartwig, G. Link, C. Raubach, J. Pereira, R. Picoloto, M. Gonçalves, N. Carreño and et al., "Synthesis and characterisation of carbon nanocomposites. In NanoCarbon 2011 (pp. 33-47). Springer, Berlin, H," in *NanoCarbon 2011*, Berlin, Heidelberg, 2013.
- [159] H. Yang, G. Xu, X. Wei, J. Cao, L. Yang and P. Chu, "Ultrafast hetero-assembly of monolithic interwoven V<sub>2</sub>O<sub>5</sub> nanobelts/carbon nanotubes architectures for high-energy alkali-ion batteries," *Journal of Power Sources*, vol. 395, pp. 295-304, 2018.
- [160] E. Brown, S. Park, A. Elangovan, Y. Yuan, J. Kim, X. Sun, X. Zhang, G. Wang and et al., "Facilitating high-capacity V<sub>2</sub>O<sub>5</sub> cathodes with stable two and three Li<sup>+</sup> insertion using a hybrid membrane structure consisting of amorphous V<sub>2</sub>O<sub>5</sub> shells coaxially deposited on electrospun carbon nanofibers," *Electrochimica Acta*, 269, pp.144-154., vol. 269, pp. 144-154, 2018.
- [161] L. Zhou, D. Zhao and X. Lou, "LiNi<sub>0.5</sub>Mn<sub>1.5</sub>O<sub>4</sub> hollow structures as high-performance cathodes for lithium-ion batteries," *Angewandte Chemie International Edition*, vol.51, no.1, pp. 239-241, 2012.
- [162] Q. Qu, L. Fu, X. Zhan, D. Samuelis, J. Maier, L. Li, S. Tian, Z. Li and et al., " and Wu, Y., 2011. Porous LiMn<sub>2</sub>O<sub>4</sub> as cathode material with high power and excellent cycling for aqueous rechargeable lithium batteries," *Energy & Environmental Science*, vol. 4, no. 10, pp. 3985-3990, 2011.
- [163] P. Nakhnivej, S. Park, K. Shin, S. Yun and H. Park, "Hierarchically structured vanadium pentoxide/reduced graphene oxide composite microballs for lithium ion battery cathodes," *Journal of Power Sources*, vol. 436, p. 226854, 2019.
- [164] J. Jiang, J. Zhu, W. Ai, Z. Fan, X. Shen, C. Zou, J. Liu, H. Zhang and et al., "Evolution of disposable bamboo chopsticks into uniform carbon fibers: a smart strategy to fabricate sustainable anodes for Li-ion batteries," *Energy & Environmental Science*, vol. 7, no. 8, pp. 2670-2679, 2014.
- [165] X. Gu, Y. Wang, C. Lai, J. Qiu, S. Li, Y. Hou, W. Martens, N. Mahmood and et al., "Microporous bamboo biochar for lithium-sulfur batteries," *Nano Research*, vol. 8, no. 1, pp. 129-139, 2015.
- [166] X. Zhang, J. Hu, X. Chen, M. Zhang, Q. Huang, X. Du, Y. Liu and X. Li, "Microtubular carbon fibers derived from bamboo and wood as sustainable anodes for lithium and sodium ion batteries," *Journal of Porous Materials*, vol. 26, no. 6, pp. 1821-1830, 2019.
- [167] M. Jiao, T. Liu, C. Chen, M. Yue, G. Pastel, Y. Yao, H. Xie, W. Gan and et al., "Holey three-dimensional wood-based electrode for vanadium flow batteries," *Energy Storage Materials*, vol. 27, pp. 327-332, 2020.
- [168] M. Chen, S. Jiang, S. Cai, X. Wang, K. Xiang, Z. Ma, P. Song and A. Fisher, "Hierarchical porous carbon modified with ionic surfactants as efficient sulfur hosts for the high-performance lithium-sulfur batteries," *Chemical Engineering Journal*, vol. 313, pp. 404-414, 2017.
- [169] H. Tan, X. Yu, K. Huang, J. Zhong and B. Lu, "Large-scale carambola-like V<sub>2</sub>O<sub>5</sub> nanoflowers arrays on microporous reed carbon as improved electrochemical performances lithium-ion batteries cathode," *Journal of Energy Chemistry*, vol. 51, pp. 388-395, 2020.
- [170] X. Liang, G. Gao, Y. Liu, Z. Ge, P. Leng and G. Wu, "Carbon nanotubes/vanadium oxide composites as cathode materials for lithium-ion batteries," *Journal of Sol-Gel Science and Technology*, vol. 82, no. 1, pp. 224-232, 2017.
- [171] X. Rui, Z. Lu, H. Yu, D. Yang, H. Hng, T. Lim and Q. Yan, "Ultrathin V<sub>2</sub>O<sub>5</sub> nanosheet cathodes: realizing ultrafast reversible lithium storage," *Nanoscale*, vol. 5, no. 2, pp. 556-560, 2013.
- [172] B. Hu, L. Li, X. Xiong, L. Liu, C. Huang, D. Yu and C. Chen, "High-performance of copper-doped vanadium pentoxide porous thin films cathode for lithium-ion batteries," *Journal of Solid State Electrochemistry*, vol. 23, no. 5, pp. 1315-1324, 2019.
- [173] Z. Huang, Z. Wang, Q. Jing, H. Guo, X. Li and Z. Yang, " Investigation on the effect of Na doping on structure and Li-ion kinetics of layered LiNi<sub>0.6</sub>Co<sub>0.2</sub>Mn<sub>0.2</sub>O<sub>2</sub> cathode material," *Electrochimica Acta*, vol. 192, pp. 120-126, 2016.
- [174] F. Schipper, M. Dixit, D. Kovacheva, M. Talianker, O. Haik, J. Grinblat, E. Erickson, C. Ghanty and et al.,

- "Stabilizing nickel-rich layered cathode materials by a high-charge cation doping strategy: zirconium-doped  $\text{LiNi}_0.6\text{Co}_0.2\text{Mn}_0.2\text{O}_2$ ," *Journal of Materials Chemistry A*, vol. 4, pp. 16073-16084, 2016.
- [175] L. Xue, Y. Li, B. Xu, Y. Chen, G. Cao, J. Li, S. Deng, Y. Chen and et al., "Effect of Mo doping on the structure and electrochemical performances of  $\text{LiNi}_0.6\text{Co}_0.2\text{Mn}_0.2\text{O}_2$  cathode material at high cut-off voltage," *Journal of Alloys and Compounds*, vol. 748, pp. 561-568, 2018.
- [176] L. Ma, L. Mao, X. Zhao, J. Lu, F. Zhang, P. Ding, L. Chen and F. Lian, "Improving the Structural Stability of Li-Rich Layered Cathode Materials by Constructing an Antisite Defect Nanolayer through Polyanion Doping," *ChemElectroChem*, vol.4, pp.3068-3074, 2017.
- [177] Y. Zhao, J. Liu, S. Wang, R. Ji, Q. Xia, Z. Ding, W. Wei, Y. Y. Liu and et al., "Surface Structural Transition Induced by Gradient Polyanion-Doping in Li-Rich Layered Oxides: Implications for Enhanced Electrochemical Performance," *Advanced Functional Materials*, vol. 26, pp. 4760-4767, 2016.
- [178] Y. Zhang, T. Ren, J. Zhang, J. Duan, X. Li, Z. Zhou, P. Dong and D. Wang, "The role of boracic polyanion substitution on structure and high voltage electrochemical performance of Ni-Rich cathode materials for lithium ion batteries," *Journal of Alloys and Compounds*, vol. 805, pp. 1288-1296, 2019.
- [179] Q. Xie, W. Li, A. Dolocan and A. Manthiram, "Insights into boron-based polyanion-tuned high-nickel cathodes for high-energy-density lithium-ion batteries," *Chemistry of Materials*, vol. 31, no. 21, pp. 8886-8897, 2019.
- [180] M. Kim, M. Avdeev and B. Kang, "Multielectron-Capable Li-Rich Polyanion Material with High Operating Voltage:  $\text{Li}_5\text{V}_2\text{PO}_4\text{F}_8$  for Li-Ion Batteries," *ACS Energy Letters*, vol. 5, no. 2, pp. 403-410, 2019.
- [181] L. Qiu, W. Xiang, W. Tian, C. Xu, Y. Li, Z. Wu, T. Chen, K. Jia and et al., "Polyanion and cation co-doping stabilized Ni-rich Ni-Co-Al material as cathode with enhanced electrochemical performance for Li-ion battery," *Nano Energy*, vol.63, p.103818, 2019.
- [182] A. Padhi, K. Nanjundaswamy and J. Goodenough, "Phospho-olivines as positive-electrode materials for rechargeable lithium batteries," *Journal of the electrochemical society*, vol. 144, no. 4, p. 1188, 1997.
- [183] J. Lu, S. Nishimura and A. Yamada, "Polyanionic solid-solution cathodes for rechargeable batteries," *Chemistry of Materials*, vol.29, no.8, pp.3597-3602, 2017.
- [184] A. Padhi, V. Manivannan and J. Goodenough, "Tuning the position of the redox couples in materials with NASICON structure by anionic substitution," *Journal of the Electrochemical Society*, vol. 145, no. 5, p. 1518, 1998.